

PART I

INVESTIGATIONS OF THE MECHANISM AND KINETICS OF THE  
FORMATION OF MALACHITE GREEN DYE

- A. MECHANISM OF THE OXIDATION OF  
LEUCO MALACHITE GREEN
- B. KINETICS OF THE CONVERSION OF  
MALACHITE GREEN CARBINOL TO DYE

PART II

DETERMINATION OF SOME MOLECULAR STRUCTURES BY THE  
METHOD OF ELECTRON DIFFRACTION

- A. ADAMANTANE
- B. 1,3,5,7,-CYCLOOCTATETRAENE

PART III

THE MOLECULAR STRUCTURE OF ARSENOBENZENE. DETERMINATION  
OF THE UNIT CELL AND SPACE GROUP OF THE CRYSTAL

Thesis by

Kenneth W. Hedberg

In Partial Fulfilment of the Requirements for the Degree of  
Doctor of Philosophy, California Institute of Technology,  
Pasadena, California, 1948

TABLE OF CONTENTS

Page

Acknowledgement

Abstract

Part I

Investigations of the Mechanism and Kinetics  
of the Formation of Malachite Green Dye

A.	Mechanism of the Oxidation of Leuco Malachite Green. . . . .	1
	Introduction . . . . .	1
	Experimental . . . . .	5
	(a) Reagents . . . . .	5
	(b) Procedure. . . . .	7
	Results. . . . .	9
	Discussion of Curves . . . . .	12
	(a) Malachite Green Dye. . . . .	12
	(b) Oxidized Leuco Malachite Green . . . . .	12
	(c) Malachite Green Carbinol . . . . .	15
	Discussion . . . . .	15
	(a) Possible Mechanisms for the Oxidation. . . . .	15
	(b) Consideration of the Oxidation of Ethanol. . . . .	17
B.	Kinetics of the Conversion of Malachite Green Carbinol to Dye. . . . .	19
	Experimental . . . . .	19
	Results. . . . .	21
	Discussion . . . . .	23

TABLE OF CONTENTS (Cont.)

	<u>Page</u>
References to Part I. . . . .	35

Part II

Determination of Some Molecular Structures  
by the method of Electron Diffraction

General Introduction. . . . .	36
A. Adamantane . . . . .	39
Introduction . . . . .	39
Experimental . . . . .	39
Radial Distribution Curve. . . . .	41
Correlation of Visual and Intensity Curves . . . . .	43
Conclusions. . . . .	45
B. 1,3,5,7-Cycloöctatetraene. . . . .	47
Introduction . . . . .	47
Experimental . . . . .	48
Radial Distribution Curve. . . . .	48
Theoretical Intensity Curves . . . . .	52
Correlation of Visual and Calculated Intensity Curves . . . . .	56
Electronic Structure of Cyclooctatetraene and Choice of a Best Model . . . . .	60
References. . . . .	65

Part III

The Molecular Structure of Arsenobenzene. Determination  
of the Space Group and Unit Cell of the Crystal

Introduction . . . . .	67
Preparation of Arsenobenzene Crystals. . . . .	68

TABLE OF CONTENTS (Cont.)

	<u>Page</u>
Physical Characteristics of The Crystals. . . . .	71
A. Optical Examination . . . . .	71 ✓
B. Cleavage. . . . .	71
Determination of a Tentative Unit Cell. . . . .	74
A. Laue Symmetry . . . . .	74
B. Layer Line Measurements . . . . .	74
Precise Determination of Lattice Constants. . . . .	75
Verification of the Unit Cell . . . . .	75
Number of Molecules per Unit Cell . . . . .	80
Determination of the Space Group of Arsenobenzene . . . . .	80
Summary of Work on Arsenobenzene. . . . .	82
Discussion. . . . .	84
References. . . . .	87

Propositions

## ACKNOWLEDGEMENT

I wish especially to express my appreciation to Professor Verner Schomaker, not only for expert advice in the electron diffraction work, but for illuminating discussions of the work on malachite green and of numerous other scientific problems which have presented themselves in the past many months. Thanks also go to Dr. C. Gardner Swain, who suggested the work on malachite green; to Dr. Jürg Waser, who assisted with the X-ray diffraction work on arsenobenzene; and to Dr. Werner Nowacki for assistance in the electron diffraction investigation of adamantane. I am further indebted to Dr. Robert B. Corey for valuable suggestions about the crystal structure work, and for much helpful advice regarding the preparation of this thesis. Lastly, I wish to thank my wife for her continued patience and encouragement throughout the course of my graduate studies and research at the Institute.

**ABSTRACT**

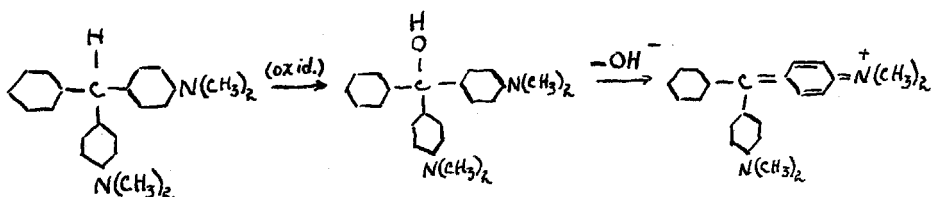
# ABSTRACT

## Part I

### INVESTIGATIONS OF THE MECHANISM AND KINETICS OF THE FORMATION OF MALACHITE GREEN DYE

#### A. Mechanism of the Oxidation of Leuco Malachite Green

The oxidation of leuco malachite green to malachite green dye is commonly considered to take place through the formation of malachite green carbinol:



The present study shows that malachite green carbinol cannot be an intermediate in this process. The proof rests on the observation that the oxidation of leuco malachite green to dye occurs at a much more rapid rate than that at which malachite green carbinol is dehydrated to dye.

It is suggested that this result is evidence that the oxidation of ethanol does not take place through the formation of a gem-diol as intermediate.

#### B. Kinetics of the Conversion of Malachite Green Carbinol to Dye

The kinetics of the conversion of malachite green carbinol to dye have been studied in solutions of ionic strength approximately 2.84 over the pH range 2.5 - 4.9.

The rate constants representing the rate of approach to equilibrium are first order with respect to carbinol and have the values 15.8, 13.4, 6.2, 8.7, 21.4 and  $20.4 \times 10^{-4}$   $\text{sec}^{-1}$  at pH 4.88, 4.69, 4.08, 2.98, 2.25, and 1.65, respectively.

An attempt is made to account for the observed minimum in the curve which results when these values of the constant for the approach to equilibrium are plotted against pH.

## Part II

### DETERMINATION OF SOME MOLECULAR STRUCTURES BY THE METHOD OF ELECTRON DIFFRACTION

#### A. Adamantane

An investigation of the structure of adamantane by electron diffraction has led to the following results for the structural parameters:  $\text{C} - \text{C} = 1.54 \pm 0.01 \text{ \AA}$ ,  $\angle \text{C}_2\text{C}_3\text{C}_2 = 109.5 \pm 1.5^\circ$ ,  $\text{C} - \text{H} = 1.09 \text{ \AA}$ . (assumed),  $\angle \text{HCH} = 109^\circ 28'$  (assumed) The molecular symmetry  $T_d - \bar{4}3m$  was assumed. These results are in agreement with results obtained from x-ray diffraction studies of the crystal.

#### B. 1,3,5,7 - cyclooctatetraene

The structure of cyclooctatetraene is of great theoretical importance to chemists because of the relationship between this molecule and the benzene molecule. From an earlier electron diffraction investigation of cyclooctatetraene it was concluded that all C - C bonded distances were equal



and that the molecule has the symmetry  $D_{4d}$ : This result is in complete disagreement with preliminary results from an x-ray diffraction investigation currently in progress in another laboratory; these results indicate cyclooctatetraene to have two different C - C bonded distances and the molecular symmetry  $D_{2d}$ .

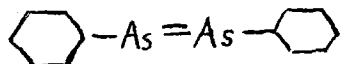
The results of our electron diffraction investigation show that cyclooctatetraene has two C - C bonded distances, which are about equal to the normal double bond distance and to the conjugated single bond distance. The molecule has the symmetry  $D_{2d}$  "tub" in agreement with the result from x-ray diffraction.

The positions of the double bonds in the molecule cannot be placed from the electron diffraction data; two different regions of parameter combinations, depending upon the position of the double bonds, give acceptable models. It is possible to make a choice between these regions, however, based upon considerations of strains induced by rotation about the double bond. The structural parameters for the best model in the chosen region are: C - C =  $1.43(5) \pm 0.03\overset{\circ}{\text{Å}}$ , C = C =  $1.33 \pm 0.02\overset{\circ}{\text{Å}}$ ,  $\angle \text{CCG} = 126.5^\circ \pm 1.5^\circ$ ,  $\angle \text{CCH} = 126.5 \pm 1.5^\circ$  (assumed), and C - H =  $1.09\overset{\circ}{\text{Å}}$ , (assumed).

### Part III

#### THE MOLECULAR STRUCTURE OF ARSENOBENZENE DETERMINATION OF THE SPACE GROUP AND UNIT CELL

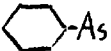
The molecular formula of arsenobenzene is commonly written as



although the true molecular formula is unknown. Determinations of the molecular weight of this substance indicate from 2 to 6 of the  $\text{C}_6\text{H}_5\text{As}$  units to be combined in solution. It was hoped that a determination of the space group and unit cell of the crystal would yield useful information regarding the structure of the molecule.

A tentative unit cell was determined from layer line measurements made from rotation photographs, and verified by a symmetrical Laue photograph. The arsenobenzene crystal was found to be monoclinic; and to contain 12  $\text{C}_6\text{H}_5\text{As}$  units per cell. Accurate values of the lattice constants were obtained from oscillation photographs. These values are  $a_1 = 12.16 \pm 0.02 \text{ \AA.}$ ,  $a_2 = 6.22 \pm 0.01 \text{ \AA.}$ ,  $a_3 = 24.10 \pm 0.08 \text{ \AA.}$ ,  $\alpha_2 (= \beta) = 110^\circ 14' \pm 5'$ . With the aid of Weissenberg photographs the probable space group of the crystal was determined to be  $C_{2h}^4 - P_c^2$  or  $C_s^2 - P_c$ .

The space group and unit cell of arsenobenzene together with considerations based on the chemistry of arsenic allow interesting deductions to be made regarding the molecules

of this substance. One molecule may consist of 2,3, or 6  
 units, giving 6,4, or 2 molecules per unit  
cell, respectively. There is, however, considerable quali-  
tative evidence which indicates that discrete molecules of  
arsenobenzene do not exist in the crystal, and that instead  
the arsenic atoms are bonded together in infinite chains,  
probably parallel to the monoclinic axis.

**Part I**

**INVESTIGATIONS OF THE MECHANISM AND KINETICS OF THE  
FORMATION OF MALACHITE GREEN DYE**

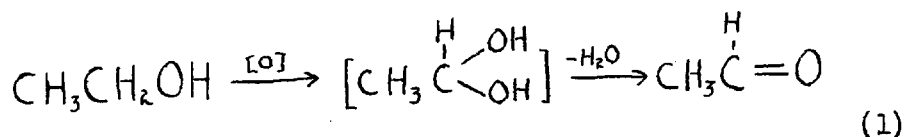
- A. MECHANISM OF THE OXIDATION OF  
LEUCO MALACHITE GREEN**
  
- B. KINETICS OF THE CONVERSION OF  
MALACHITE GREEN CARBINOL TO DYE**

MECHANISM OF THE OXIDATION OF LEUCO MALACHITE GREEN

Introduction

Although the oxidation of C-H bonds in aqueous solution with powerful oxidizing agents such as potassium permanganate or ceric salts is common practice in organic chemistry, the mechanism of the oxidation process is not clearly understood. The more important mechanisms which have been proposed may be conveniently considered in two classifications, depending upon whether the primary step is the removal of a neutral atom from the reducing agent, or the simple transfer of electrons from the reducing agent to the oxidizing agent. In mechanisms falling into either of these classifications the substances formed from the initial step are generally intermediates, which undergo subsequent reactions of various types to give the final products.

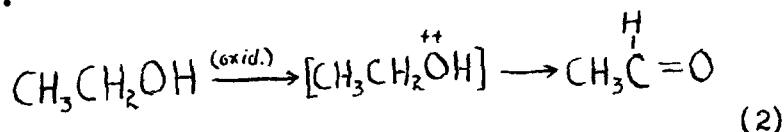
As an example of a mechanism in the first group, we may consider the oxidation of ethanol to acetaldehyde, as it is presented in many textbooks<sup>(1)</sup>



The initial step here may be visualized as the abstraction by the oxidizing agent of a neutral hydrogen atom from the hydroxylated carbon atom; this step is followed by the

attachment of a hydroxyl radical to yield the gem-diol intermediate, and finally, by dehydration of the latter to give acetaldehyde. Of course, a mechanism which involves the abstraction of hydrogen atoms from ethanol need not necessarily form the diol as intermediate; instead of one, two hydrogen atoms may be removed and acetaldehyde formed directly by shifts of electrons within the molecule.

The oxidation of ethanol may also be used to illustrate the second type of mechanism, in which the primary step is a simple electron transfer from the reducing to the oxidizing agent.



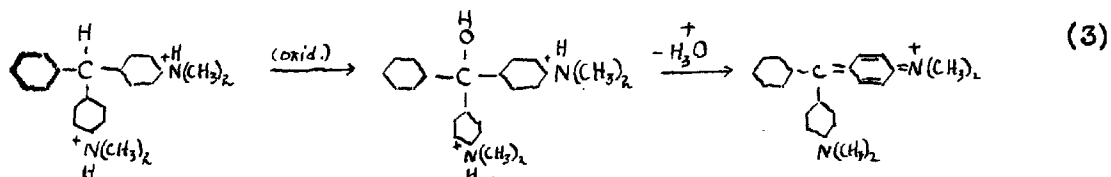
In this process the oxidizing agent may be considered to attack the oxygen atom and remove an unshared pair of electrons. This step is followed by the loss of two protons from the resulting ion to give acetaldehyde.

In comparison with the simple electron transfer, the abstraction of hydrogen atoms as a process of oxidation has been recognized for only a relatively short time.<sup>(2)</sup> It is now known to be of fundamental importance in organic reactions such as autooxidations, induced polymerizations, and others. Recently, many chemists have come to believe that, in organic reactions, dehydrogenation mechanisms of oxidation are even

more important than simple electron transfer mechanisms. In support of this idea, Waters<sup>(3)</sup> found that many powerful oxidizing agents, when dissolved in hydrocarbons, catalyze the absorption of oxygen by these hydrocarbons. Presumably the oxidizing agent abstracts a hydrogen atom from an organic molecule which then combines with oxygen to give a peroxy free radical. This free radical abstracts a hydrogen atom from a second hydrocarbon molecule and a chain reaction is thus initiated. The action of the oxidizing agent in this process suggests that such substances may behave in general as dehydrogenators in their reactions.

The problem of determining whether an oxidation in aqueous phase takes place by a dehydrogenation or a simple electron transfer as primary process is an exceedingly difficult one. Both classifications contain possible mechanisms which can give rise to identical products, and the ability to make a decision in favor of one type of mechanism usually depends upon establishing the identity of a highly transitory intermediate. In the case of the leuco triphenylmethane dyes, however, the initial products to be expected from some of the different oxidation mechanisms are not transitory intermediates, but are stable chemical compounds which may be easily identified. The oxidation of these leuco dyes in acid solution has generally been regarded as yielding first the carbinols, or "color bases", which are

subsequently dehydrated to the equilibrium quantity of dye. (4)



leuco malachite  
green (colorless)

malachite green  
carbinol (colorless)

malachite green  
dye (green to  
blue-green)

This mechanism is somewhat analogous to (1) in that the primary oxidation product is formed by the conversion of a hydrogen atom into a hydroxyl group, and, like (1), may be considered as involving the formation of free radicals as a primary step. Moreover, it would seem to be a very logical mechanism, since the triphenylmethane dyes are known to give free radicals (5) and the oxidation of triphenylmethane (with nitric acid) leads to triphenyl carbinol. The formation of malachite green dye from the leuco base by a free radical process involving the abstraction of two hydrogen atoms or by an electronic process analogous to (2) is also possible. In these cases, however, the carbinol would not be expected as intermediate.

The primary objective of this study, then, was to obtain information about the products resulting from the oxidation of leuco malachite green, and from such information to deduce the mechanism by which the oxidation takes place. Secondly,



it was felt that the results obtained would provide some basis for predictions regarding the mechanism of oxidation of certain other organic compounds.

### Experimental

The experimental part of the investigation consisted of measurements of the rate of color development in acid solutions of ceric ion and leuco base, and their comparison with measurements made on carbinol solutions and dye solutions under appropriately similar conditions. Ceric ion was chosen as the oxidizing agent because of its high electrochemical potential and the negligible color of it and cerous ion at the concentrations used. The results obtained prove conclusively that malachite green carbinol is not an intermediate in the oxidation of the leuco base to dye. The proof rests on the observation that the formation of dye from carbinol occurs at a slower rate than that at which leuco base is oxidized to dye.

#### A. Reagents

Two samples of leuco base were used. The first sample was the lowest melting allotrope; its melting point, 92-93°C, compares well with the melting point 93-94°C, previously reported.<sup>(6)</sup> It was obtained by recrystallizing 5g. of a crude product twice from 50 ml. of 95% ethanol, once from a benzene-ethanol mixture, and finally from ligroin, and drying.

Solutions of this material less than about one day old were satisfactory, but the aged solutions gave only a small fraction of the expected color when mixed with acid ceric sulfate. The reason for this behavior is not known. The second sample was an Eastman Kodak Company product with a m.p. 102-103°C. Solutions of this material were stable in air indefinitely, whether the sample was recrystallized first or not.

Two stock solutions of malachite green dye (the terms "malachite green" and "malachite green dye" will be used interchangeably in the following pages and refer to the singly positively charged cation) were used in the experiments, and gave similar kinetic results. The first of these was made up by dissolving National Aniline certified grade malachite green oxalate in distilled water which had been made acid to about pH 5 with sulfuric acid. The second was made from the same source material, but involved first the preparation of the carbinol. Six grams of the oxalic acid salt were dissolved in 660 cc. distilled water and the carbinol base precipitated by adding 60 cc. of 1M. sodium hydroxide. This precipitate was filtered off and recrystallized twice from 95% ethanol containing a trace of dissolved potassium hydroxide. It was then washed cautiously with ether and finally recrystallized from ligroin. After drying, the resulting material had a melting point of 121-121.5°C., which compares well with the value 120-122°C previously reported for the higher melting allotrope. (7)

All other materials used, ceric bisulfate,  $\text{Ce}(\text{HSO}_4)_4$  (from G. F. Smith); ammonium sulfate; cerous nitrate hexahydrate,  $\text{Ce}(\text{NO}_3)_3 \cdot 6\text{H}_2\text{O}$ ; and sulfuric acid, were reagent grade.

B. Procedure

In order to obtain conclusive evidence regarding the primary oxidation product, it was necessary to examine the behavior of malachite green carbinol and malachite green dye under conditions as nearly as possible identical with those existing in the solutions of oxidized leuco malachite green. All experiments were made in aqueous media of ionic strength  $2.38 \pm 0.02$  ( $= \frac{1}{2} \sum C_i Z_i^2$ ). For leuco malachite green the following procedure was used: Exactly 1.0 ml. of 0.001M. leuco base in 0.01 M. sulfuric acid was placed in a cylindrical Klett colorimeter tube of about 15 ml. capacity. The oxidizing solution, consisting of 2.0 ml. 0.001 M. ceric tetrabisulfate in 0.02 M. sulfuric acid, 2.7 ml. 3.29 M. ammonium sulfate, and 6.3 ml. distilled water, was made up in a separate tube immediately before using. The pH of the reaction mixtures was varied as desired by adding sulfuric acid or sodium hydroxide to the oxidizing solution before mixing and diminishing the distilled water by an equal amount. After both solutions had been brought to  $24^\circ\text{C}$ , the oxidizing solution was poured into the leuco base, the resulting mixture shaken, and measurements of the color intensity made at intervals with a Klett-Sommerson photoelectric colorimeter equipped with a red filter. The reaction mixture was kept

in a thermostat at  $24.0 \pm 0.1^{\circ}\text{C}$ . at all times when measurements were not being made. At the conclusion of each run the pH of the reaction mixture was measured by a Beckmann pH meter and a glass electrode.

The procedure for malachite green dye was the same as that for the leuco base, except that in place of the oxidizing ceric sulfate solution a solution having the same concentration of cerous nitrate was used.

The procedure for malachite green carbinol had to be modified slightly because the solubility of this compound in the aqueous alkaline medium necessary to prevent the formation of dye was considerably less than the 0.001 M. concentration needed for a stock solution. Instead of a stock solution, one of dye was used, and the carbinol prepared in the reaction vessel by the addition of alkali to the proper amount of dye at the time of the experiment. The cerous nitrate solution (2.0 ml. of 0.001 M. cerous nitrate hexahydrate in 0.02 M. sulfuric acid) was placed in a Klett colorimeter tube together with 0.2 ml. 0.1 N. sulfuric acid and 2.7 ml. of the ammonium sulfate solution. In another vessel was placed 1.0 ml. 0.001 M. malachite green dye, 0.2 ml. 0.1 N. sodium hydroxide, and 5.9 ml. distilled water. The pH of the resulting reaction mixture was varied when desired as described for the leuco base. About 45 minutes was allowed for the formation of carbinol before mixing the solutions; at the end of

this time the dye solution had become colorless, and although it was sometimes turbid, addition of the acid salt solution always clarified it immediately. The rate of re-solution of carbinol can not have been of any importance in the rate of this control reaction, as will become evident later from the kinetic results obtained.

### Results

Figures 1 and 2 show the behavior of leuco malachite green, malachite green carbinol, and malachite green dye under appropriately similar experimental conditions; curves are given for pH  $3.00 \pm 0.03$  and  $3.60 \pm 0.03$ . In the curves for carbinol and dye at pH 3.6 ceric ion instead of cerous ion was present, but it was found that within experimental error this substitution had no effect on the colorimeter reading. From the curves it is clear that the primary product of the oxidation of leuco malachite green cannot be the carbinol; the curves showing the development of color from carbinol and oxidized leuco base solutions are completely dissimilar. In the case of the carbinol the formation of color occurs in a regular fashion, while the curve for oxidized leuco base shows two distinct phases of color development and passes through a maximum. The curves for these two substances and the solution of dye approach the same final colorimeter reading, within experimental error; the oxidation of leuco base is thus shown to be quantitative.

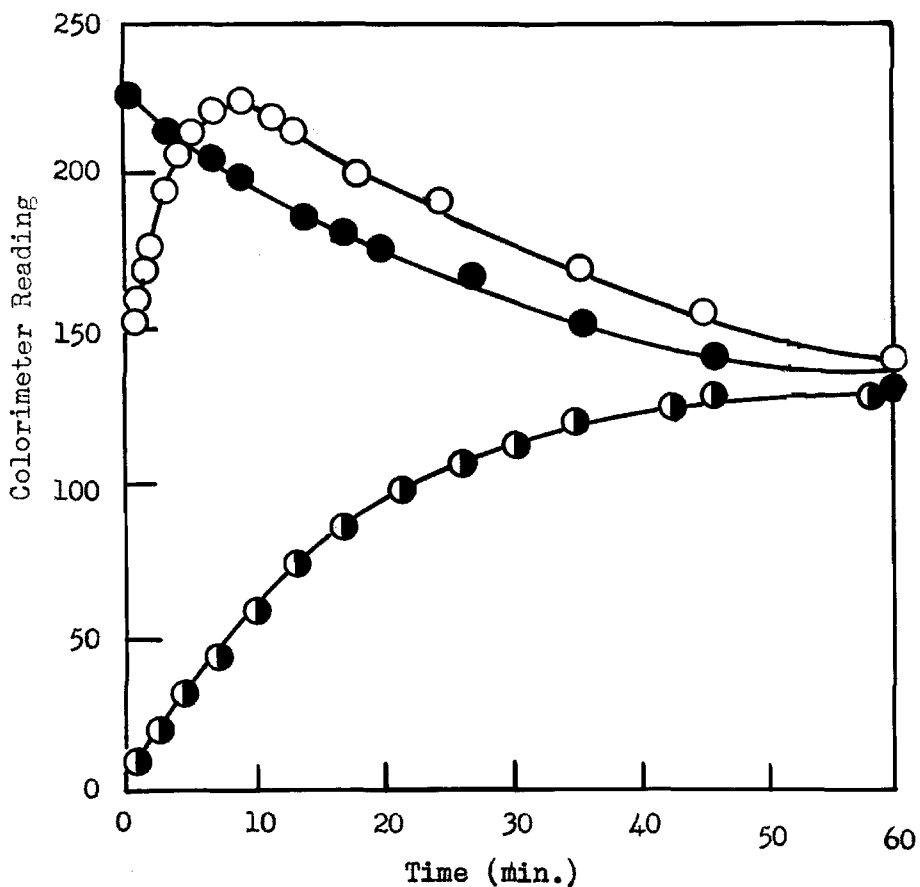


Figure 1

Development of Color in Solutions of  
Leuco Malachite Green, Malachite Green  
Carbinol, and Malachite Green Dye at  
pH  $3.00 \pm 0.03$

- $9.1 \times 10^{-5}$  M. leuco malachite green,  
 $1.82 \times 10^{-4}$  M. ceric ion
- $9.1 \times 10^{-5}$  M. carbinol base,  
 $1.82 \times 10^{-4}$  M. cerous ion
- $9.1 \times 10^{-5}$  M. malachite green,  
 $1.82 \times 10^{-4}$  M. cerous ion

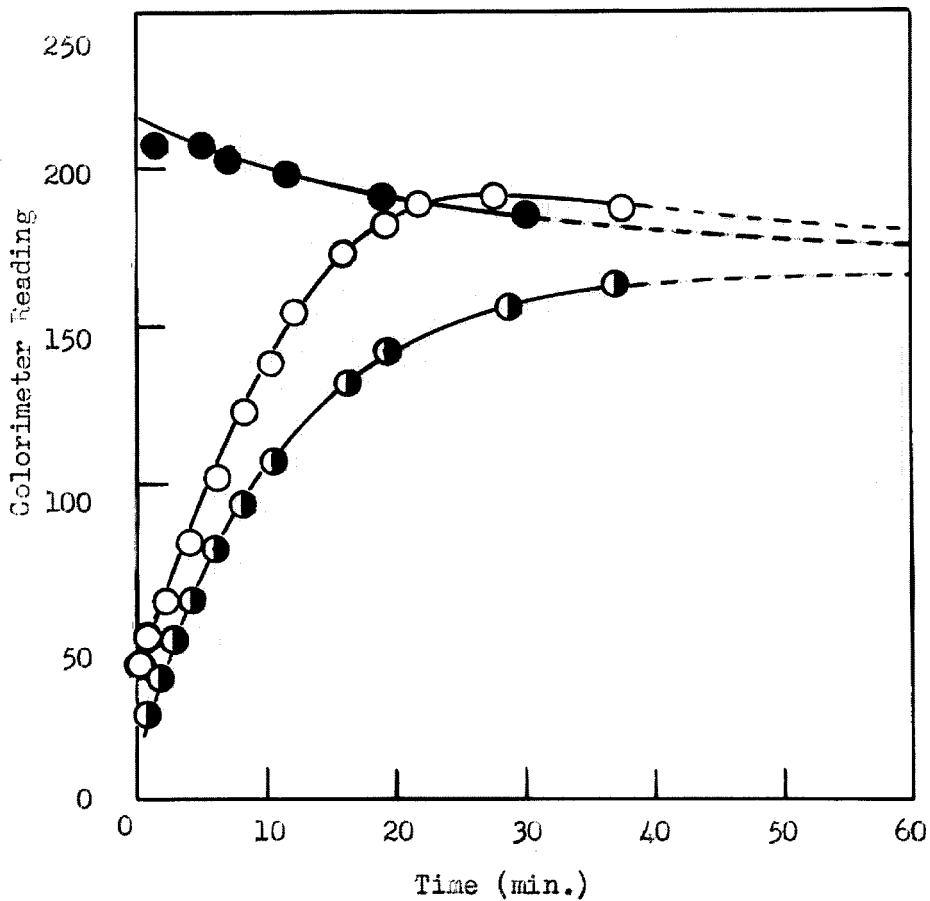


Figure 2

Development of Color in Solutions of  
Leuco Malachite Green, Malachite Green  
Carbinol, and Malachite Green Dye at  
pH  $3.60 \pm 0.03$

○  $9.1 \times 10^{-5}$  M. leuco malachite green,  
 $1.82 \times 10^{-4}$  M. ceric ion

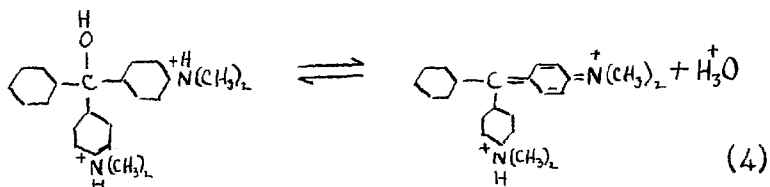
◐  $9.1 \times 10^{-5}$  M. carbinol base,  
 $9.1 \times 10^{-5}$  M. ceric ion

●  $9.1 \times 10^{-5}$  M. malachite green dye  
 $9.1 \times 10^{-5}$  M. ceric ion

Discussion of Curves

A. Malachite Green Dye.

The curves for malachite green dye shows the color of the solution to diminish with time, approaching a final value of about 60% of that initially observed at pH 3.0 and 80% at pH 3.6. No attempt was made to interpret the data kinetically, since the results are not important to the primary objective of this investigation. It may be mentioned, however, that the fading exhibited by the triphenylmethane dyes in acid solution is well known, and has been studied by several investigators<sup>(8,9)</sup>. It represents a shift of the carbinol-dye equilibrium (Equation (4) ) toward carbinol.



B. Oxidized Leuco Malachite Green

The curves for oxidized leuco malachite green show an initial rapid development of color followed by a subsequent very much slower development.\* This phenomenon is doubtless

---

\* It should be explained that, so far as the appearance of these curves is concerned, the initial rapid development of color is practically instantaneous. The appearance of color in this rapid phase could be followed by eye, but by the time the first reading on the colorimeter could be made (about 20 seconds after mixing the oxidizing solution and the solution of leuco base) the color intensity was relatively high.



due to some characteristic of tetravalent cerium. This was shown by experiments in which iodide ion was oxidized in the presence of starch as indicator under conditions similar to those used with the leuco base; two phases of color development were observed with the fraction of total color immediately formed decreasing with increasing pH. A representative curve, for pH 2.98, is presented in Figure 3.

There are two possible explanations of such behavior. The first, and more likely, involves the question of the solubility of tetravalent cerium under the conditions of the experiments. Although the solutions were quite clear to the eye, it is possible that substantial amounts of the ceric ion were precipitated through hydrolysis and remained suspended as particles of colloidal size. The second explanation is given by assuming that tetravalent cerium exists in solution in several different complex ions, which differ largely in their degrees of hydration and in their oxidizing abilities. The initial rapid formation of color (67% of the maximum intensity in less than 1 minute at pH 3.0, 23% at pH 3.6) would represent the exhaustion of the most active species, and the subsequent slower development of color would be representative of such processes as the formation of active species from the more highly hydrated, or the rate of oxidation of leuco base directly by the latter. Attempts to detect possible colloidal hydrolyzed ceric ion were made by measuring the intensity of light scattered from solutions

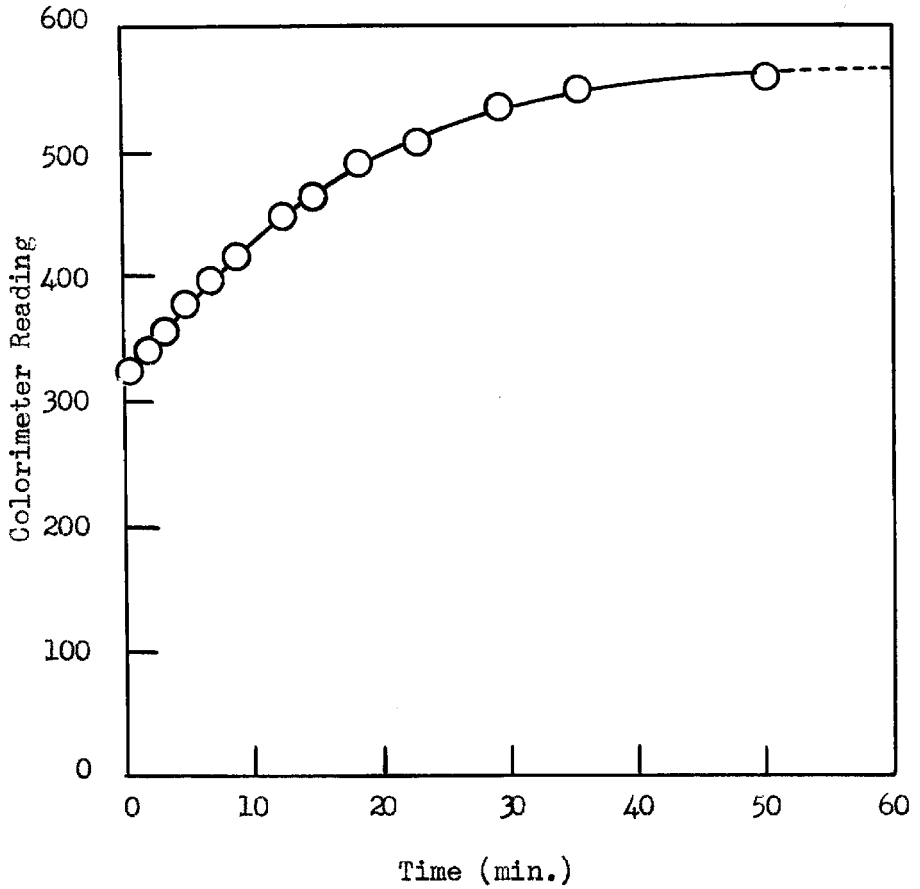


Figure 3

Oxidation of excess iodide ion  
by  $9.1 \times 10^{-3}$  M. ceric ion at  
pH 2.98 in the presence of starch  
indicator.

similar to those used in the oxidations (the leuco base was omitted) and comparing it with the intensity from control solutions. The differences found were relatively small in all cases and, because of the relatively large experimental errors, no conclusions could be drawn. It is likely, however, that special care in the preparation of the solutions, i.e., centrifugation of reagents and careful cleaning of all apparatus so as to remove dust particles, would give an answer to this interesting question.

The maximum in the curve represents the point at which dye is being formed by oxidation of leuco base at the same rate as it is being hydrated to colorless carbinol; the color intensity from this point diminishes with time and results from the hydration of dye to carbinol as shown by equation (4).

#### C. Malachite Green Carbinol

The curve for malachite green carbinol represents the approach to equilibrium in the carbinol-dye system from the carbinol side. A detailed consideration of this reaction is given in the next section of this thesis.

### Discussion

#### A. Possible Mechanisms for the Oxidation

As has already been mentioned, the oxidation of leuco malachite green has heretofore been believed to yield the carbinol, which subsequently dehydrates to the dye. The mechanism of such a reaction would doubtless involve the

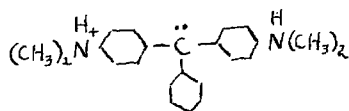
formation of an organic free radical by the abstraction of the hydrogen atom from the tertiary carbon atom and the combination of this radical with hydroxyl radicals presumably derived from the oxidizing agent. That this mechanism cannot be correct is shown by the experiments described in the preceding pages. Unfortunately, there is more than one mechanism which will satisfactorily account for the observation that leuco malachite green is oxidized directly to dye, and there appears to be no way of making a logical choice of one of these mechanisms over the others from the data available. A few of the more obvious possible mechanisms are mentioned here by way of illustration.

For the reaction in question we need consider only types of mechanisms which involve as primary steps either the abstraction of hydrogen atoms or the simple transfer of electrons. These are:

- (1) A free radical process in which two hydrogen atoms are removed from one molecule of leuco base.
- (2) A process by which only electrons are transferred from the leuco base to the oxidizing agent.
- (3) Some combination of these two processes.

In type mechanism (1) it seems reasonable to assume that one of the hydrogen atoms must be obtained from the tertiary carbon atom, since the removal of this particular atom results in an organic free radical which is stabilized by resonance among ortho and para quinoid structures. The

second hydrogen atom would almost certainly be obtained from one of the protonated nitrogen atoms, but the mechanism of its removal can only be guessed. It might require a direct attack by a molecule of oxidizing agent, but one must also consider the possibility of its just "falling off" as a consequence of the preceding attack at the tertiary carbon atom. Type mechanism (2) could take place by the removal of electrons from a nitrogen atom, or perhaps even from the tertiary carbon atom following an ionization step which would yield a carbonium ion of the form



An example of type mechanism (3) may be formulated by considering the abstraction of a hydrogen atom from the tertiary carbon atom as mentioned in the example of type (1), followed by the transfer of the odd electron to another molecule of the oxidizing agent.

#### B. Consideration of the Oxidation of Ethanol

Although the experimental evidence obtained on the oxidation of leuco malachite green is not sufficient to establish a unique mechanism for this oxidation, these data do permit some interesting conjecture regarding the mechanism of the oxidation of ethanol. For example, the results from leuco malachite green might be applied to rule our reaction (1) as

a likely mechanism for the oxidation of ethanol. Ethanol would be expected to yield free radicals with less ease than leuco malachite green because resonance stabilization of the radicals would be less; hence the formation of a gem-diol as intermediate in the case of ethanol would be even less likely than oxidation of leuco malachite green to carbinol, which does not occur.

Of course, it must be borne in mind that the discussion in the preceding paragraphs has applied only to the use of ceric ion as oxidizing agent, other oxidizing agents may act toward leuco malachite green in an entirely different way. Indeed, ceric ion has unusual complexing properties, and is known to behave in a specialized manner toward many organic compounds which possess functional groups of the type exhibited by leuco malachite green. No attempt was made in this investigation to study the action of other oxidizing agents quantitatively; however, a number of rough experiments with permanganate indicate that this agent oxidizes leuco malachite green to dye at a rate comparable to that shown in the oxidations by ceric ion. It thus appears as if the discussion above applies equally to permanganate, and it seems reasonable to suppose that other oxidizing agents may behave in a similar fashion toward leuco malachite green.

KINETICS OF THE CONVERSION OF  
MALACHITE GREEN CARBINOL TO DYE

In the course of the work on the oxidation of leuco malachite green, a number of kinetic studies were made of the formation of malachite green dye from malachite green carbinol in solutions of different hydrogen ion concentrations. The results of these investigations are described in this section.

Experimental

The determinations of rate constants were carried out for solutions of ionic strength  $2.8 \pm 1.0$  over the pH range 2-7, with a Klett-Sommerson photoelectric colorimeter equipped with a red filter. Because of the low solubility of malachite green carbinol in an alkaline medium it was necessary to prepare solutions of it at the time of the experiment by adding dilute sodium hydroxide to a solution of the dye. For this purpose a  $1.98 \times 10^{-5}$  M. stock solution of malachite green dye was made up by dissolving National Aniline certified grade malachite green oxalate in distilled water made acid to pH 5.1 with sulfuric acid. For each experiment, 4.0 ml. of 0.1 N. sodium hydroxide was added to 100 ml. of the above dye solution, and the mixture was thoroughly shaken and placed in a thermostat at  $25.0 \pm 0.03^\circ\text{C}$ . for about 45 minutes. A separate mixture containing 39.6 ml.

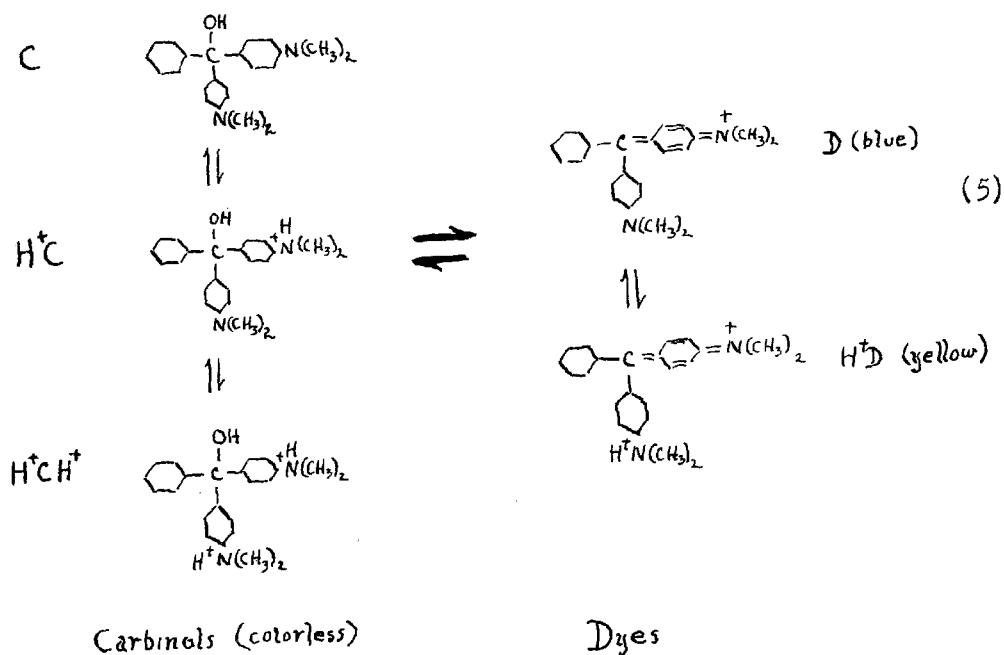
3.29 M. ammonium sulfate and 4.0 ml. sulfuric acid (of a strength depending on the pH desired in the final reaction mixture) was also made up and placed in the thermostat. Immediately before beginning the experiment 10.0 ml. of the carbinol solution was pipetted into 4.4 ml. of 3.29 M. ammonium sulfate containing no acid and a blank colorimeter reading was obtained. The acid ammonium sulfate solution was then poured into the remaining 94.0 ml. of carbinol to yield the reaction mixture from which aliquot parts were taken at intervals for measurement of the color intensity. Although the solutions of carbinol as prepared from the dye were sometimes turbid, the addition of the acid salt solution clarified them instantly. Tests showed that the rate of re-solution of carbinol could not have been the rate-determining step in the conversion of carbinol to dye up to pH 4.88, the highest pH at which experiments were made. The above procedure was used for runs above pH 4.08. At lower pH's than this, however, too large a fraction of the dye existed as the conjugate acid to permit direct measurements of the color intensity. Therefore, separate reaction mixtures were prepared for each measurement, and the solutions were buffered to pH 4 or 5 with excess citrate or acetate buffers at the end of the appropriate time interval. The development of color at the higher pH was followed for about one minute, and the curve so obtained was extrapolated back to the time of buffering for the desired value of color intensity.



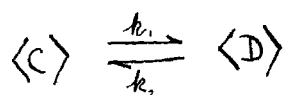
At the conclusion of each experiment the pH of the reaction mixture was measured with a Beckmann pH meter and a glass electrode. In those runs where the buffering technique was employed, the pH of one of the reaction mixtures only was measured. However, tests showed that the pH of the other mixtures of the same run was always the same, to within experimental error.

### Results

As was mentioned in the preceding section of this thesis (See p.12) malachite green carbinol and malachite green dye exist in aqueous acid solution in equilibrium with each other. Not only does there exist an equilibrium between carbinol and dye, however, but each of these substances, because of the presence of basic dimethylamino groups, is in equilibrium with its conjugate acids. The diagram (9) below illustrates these several equilibria.



The acid-base equilibria represented by the vertical arrows may be safely assumed to be fact with respect to the interconversion of carbinol and dye as represented by the horizontal arrows. With this assumption, one might expect at any given constant hydrogen ion concentration, a first order reaction scheme which can be represented by the equation



The symbols  $\langle C \rangle$  and  $\langle D \rangle$  represent all the several species of carbinol and all those of dye, respectively, and  $k_1$  and  $k_2$  are the rate constants for the forward and the back reaction. The rate constants, of course, are dependent on the hydrogen ion concentration. The expression for the rate of conversion of carbinol to dye, then has the form

$$-\frac{d\langle C \rangle}{dt} = k_1 \langle C \rangle - k_2 \langle D \rangle$$

which may be integrated\* to give

$$\ln \frac{\langle C \rangle - \langle C_\infty \rangle}{\langle C_0 \rangle - \langle C_\infty \rangle} = -(k_1 + k_2) t \quad (6)$$

where  $\langle C_0 \rangle$ ,  $\langle C_\infty \rangle$ , and  $\langle C \rangle$  represent the initial total concentration of carbinol, the concentration at equilibrium, and the concentration at any time  $t$ .

---

\*

See, for example, L. P. Hammett, "Physical Organic Chemistry", pp. 102-104, McGraw-Hill, New York, (1940).

In interpreting the results of the colorimetric measurements made in following the formation of dye from carbinol, the final colorimeter reading minus the blank reading was taken to represent the total initial concentration of carbinol ( $\langle C_0 \rangle$ ). The final colorimeter reading minus the reading at any time  $t$  was taken to represent the concentration of carbinol ( $\langle C \rangle$ ) at that time. When the experimental data were plotted in accordance with equation (6), a straight line was obtained.\* The rate curves obtained by the application of equation (6) to the data are shown in Figures 4-9. The sum of the rate constants  $k_1$  and  $k_2$  calculated from the slopes of these curves are given in Table 1 and are plotted as a function of pH in Figure 10. It is seen that as the pH decreases, the rate of approach to equilibrium at first decreases, then increases, and finally appears to level off at about pH 2. The minimum in the curve lies somewhere between pH 3 and pH 4.

### Discussion

The appearance of a minimum in the curve which results from a plot of the constant for the rate of approach to equilibrium against pH was first observed by Biddle and Porter<sup>(9)</sup> for the dehydration of malachite green carbinol;

---

\*

This result for the rate of approach to equilibrium by dehydration of carbinol is in agreement with that found by other investigators for several of the triphenylmethane dyes. (9,10,11)

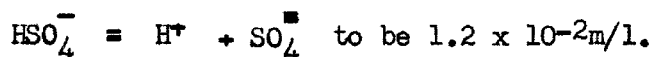
Table 1

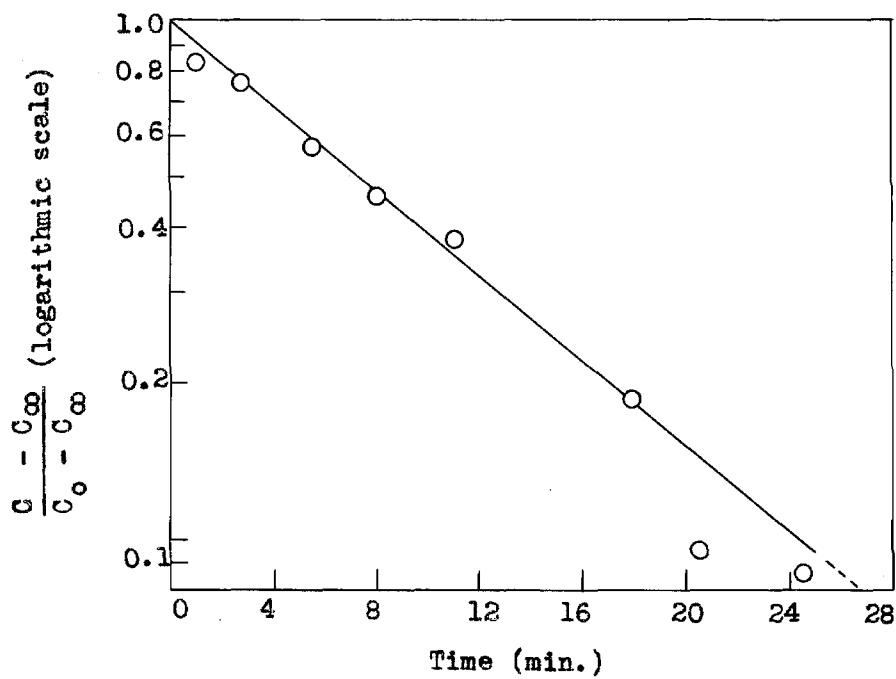
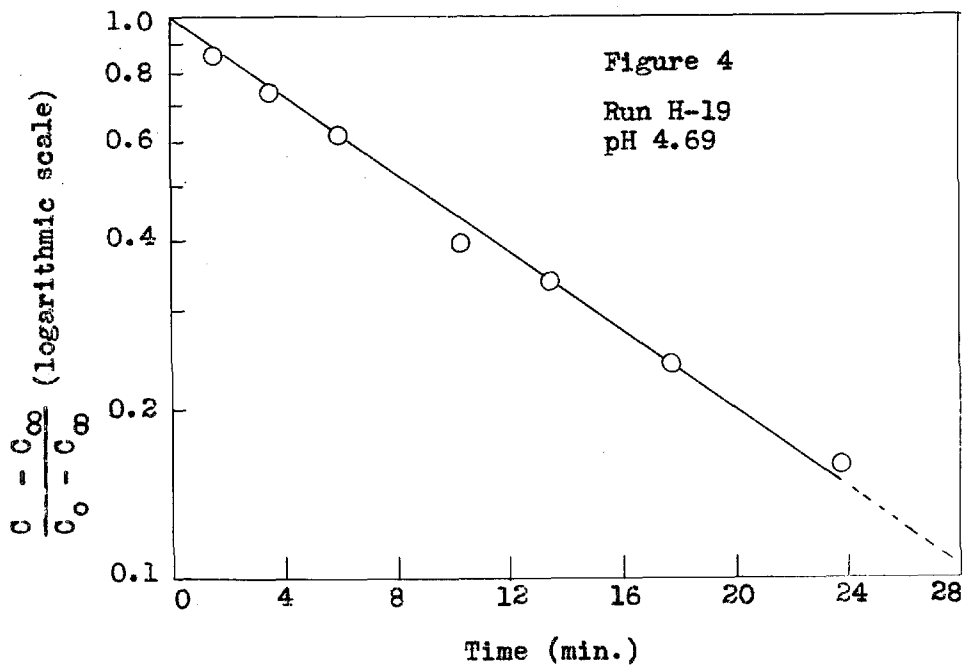
Conversion of Malachite Green Carbinol  
to Malachite Green Dye

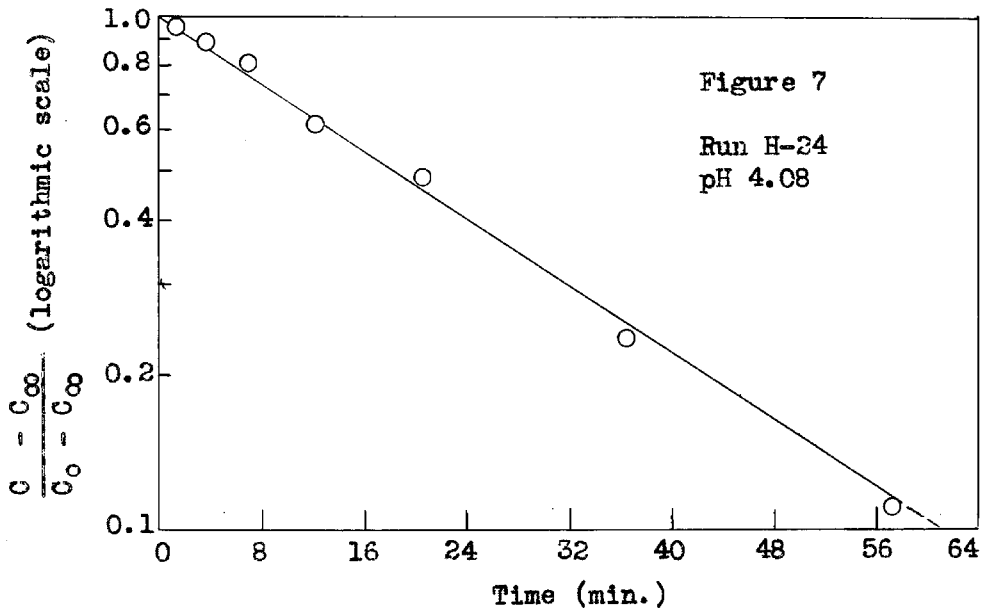
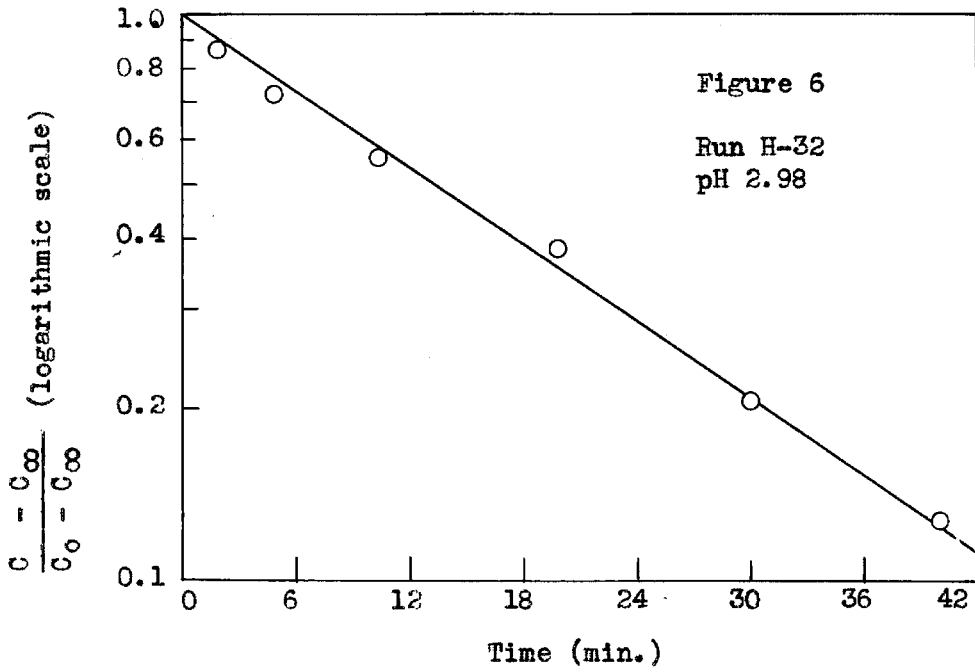
Rate of Approach to Equilibrium. Temperature  $25 \pm 0.03^\circ\text{C}$

<u>Run</u>	<u>pH of Reaction Medium</u>	<u>Ionic Strength of Reaction Medium</u>	<u>Rate Constants, <math>k_1 + k_2</math> <math>\text{sec.}^{-1} \times 10^{-4}</math></u>
H-20	4.88	2.83	15.8
H-19	4.69	2.82	13.4
H-24	4.08	2.82	6.2
H-32	2.98	2.73*	8.7
H-31	2.25	2.38*	21.4
H-30	1.65	1.91*	20.4

\* These values of ionic strength were calculated  
assuming the ionization constant of the reaction







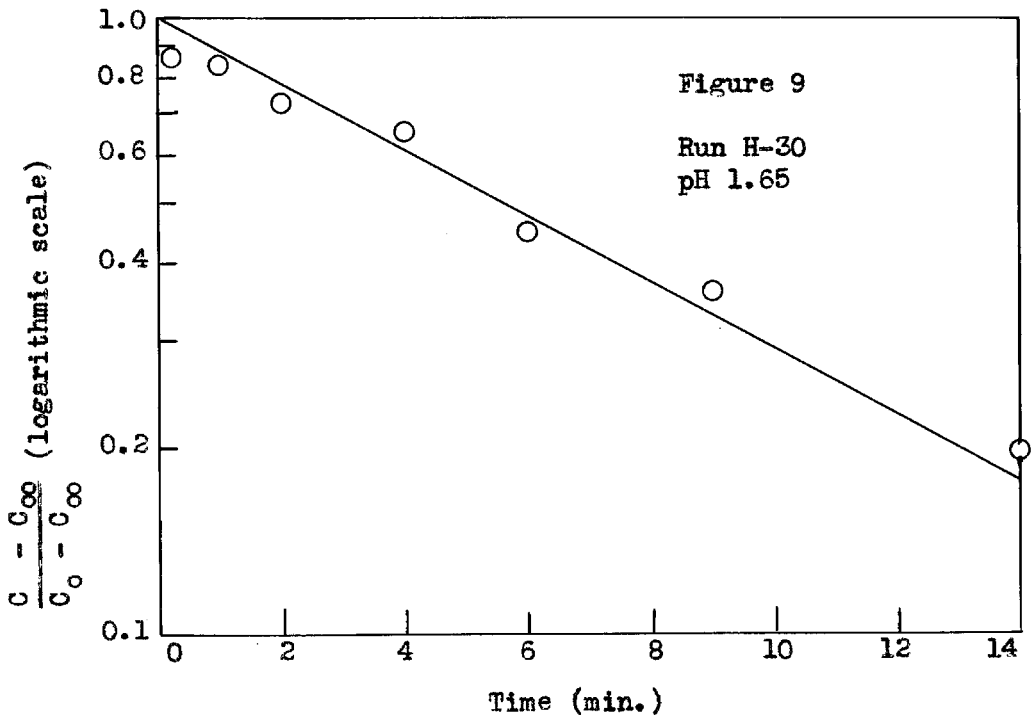
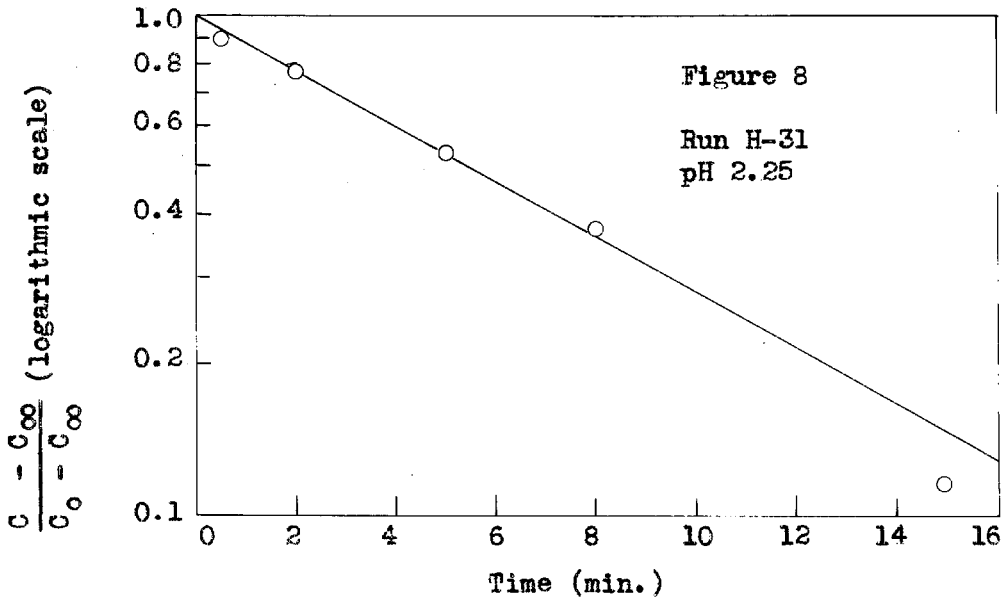
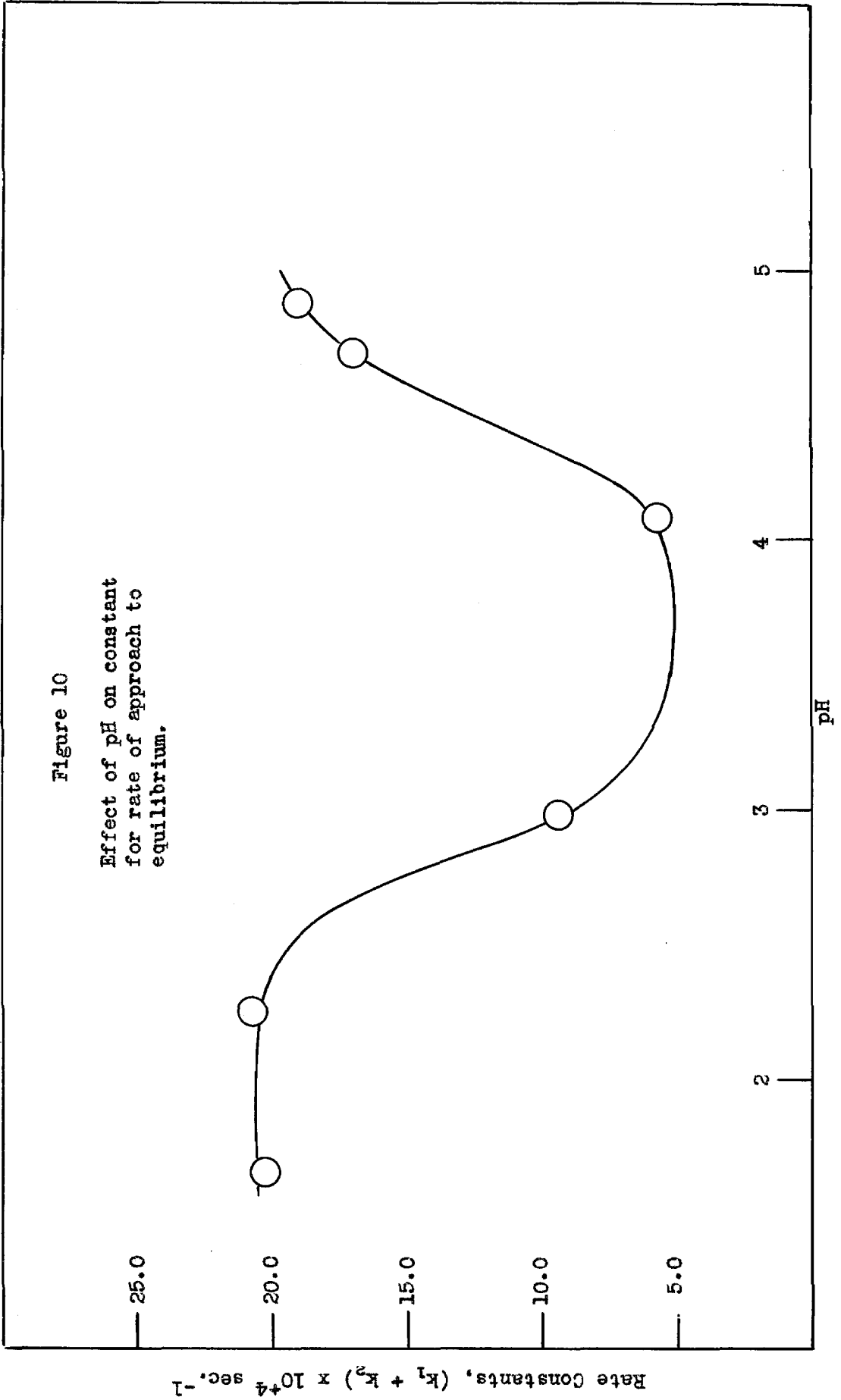


Figure 10

Effect of pH on constant for rate of approach to equilibrium.





their experiments, however, were apparently not extended to low enough pH's to show the leveling off of the curve as illustrated in Figure 10. Adams and Rosenstein<sup>(10)</sup>, for the dehydration of crystal violet carbinol, found an effect similar to that found by Biddle and Porter for malachite green carbinol. Neither of these two investigations was concerned primarily with the dehydration reaction, and a formal explanation of the effect of pH on the rate of approach to equilibrium was not made. It is clear, however, particularly from the work of Adams and Rosenstein, that the explanation lies at least in part in the complicated equilibria between protonated and unprotonated species of dye and carbinol; it further seems likely that equilibria of a similar form between carbinol and various species of the activated complex plays an important part in the explanation. In the following paragraphs an attempt is made to show how, with certain assumptions, these several equilibria can lead to the observed behavior of the rate constant for the approach to equilibrium.

According to the theory of absolute reaction rates, the rate of a chemical reaction is given by the equation

$$-\frac{dc}{dt} = C^* \frac{kT}{h} \quad (7)$$

where  $C^*$  is the concentration of the activated complex,  $k$  is Boltzmann's constant,  $h$  is Planck's constant, and  $T$  is the absolute temperature. From this equation the following

relationship for the specific reaction rate constant  $k^*$  may be found

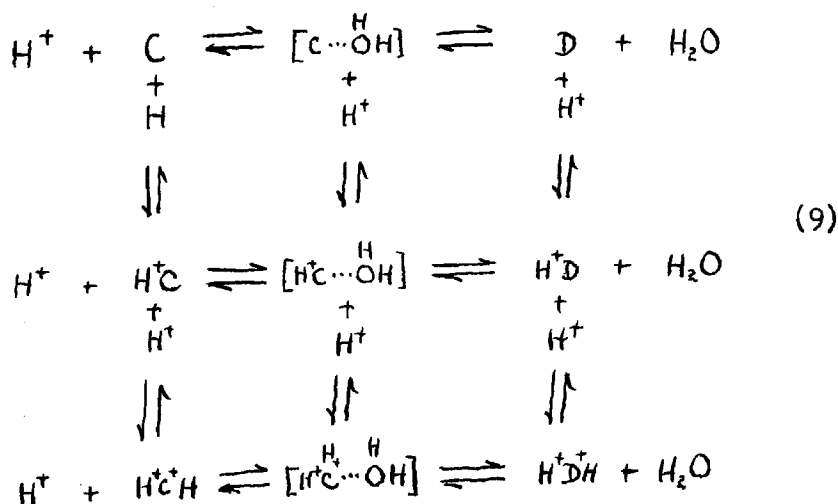
$$k^* = \frac{kT}{h} \frac{C^*}{C_A C_B \dots}$$

where  $C_A, C_B$  are the concentrations of the reacting species A, B, ... . This equation may be expressed as

$$k^* = \frac{kT}{h} K^* \tag{8}$$

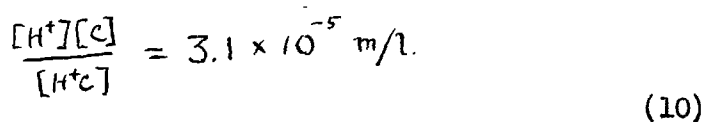
where  $K^*$  is the equilibrium constant for the reaction which is supposed to exist between the activated complex and the reactants.

In the case of the formation of malachite green dye from carbinol, it is reasonable to assume that the intermediate configuration, or activated complex, is characterized by the elongation to a critical extent of the C - O bond. The equilibria among the various species of carbinol, activated complex, and dye may then be represented by the following scheme:



where the symbols  $[C \cdots \overset{H}{OH}]$ ,  $[H^+C \cdots \overset{H}{OH}]$ , and  $[H^+C^+ \cdots \overset{H}{OH}]$  refer to the activated complex with no proton, one proton, and two protons, respectively, attached to the nitrogen atoms, and the symbols  $C$ ,  $H^+C$ ,  $H^+C^+H$ ,  $D$ , and  $H^+D$  have the meaning given them previously (See equation 5). Since it may be assumed that the rate of decomposition of the critical complex into dye or its association into carbinol is essentially independent of the number of protons which are attached to it, the behavior of the rate constant for approach to equilibrium as shown in Figure 10 must be explicable in terms of the total concentration of the activated complex, and hence of the several equilibria shown in equation (9). This behavior may be explained qualitatively by assuming that the amount of activated complex in equilibrium with unprotonated carbinol ( $C$ ) is relatively large, that in equilibrium with singly protonated carbinol ( $H^+C$ ) is smaller, and that in equilibrium with doubly protonated carbinol is again relatively large. At pH 5, where the observed rate is rapid, the concentration of  $C$  and of the activated complex  $[C \cdots \overset{H}{OH}]$  is large. As the pH decreases from 5 to 4.2, the concentration of  $H^+C$  increases at the expense of  $C$  and the amount of activated complex present diminishes; the resultant rate of approach to equilibrium is slower. At pH 4.2 the formation of the species  $H^+C^+H$  begins to be felt and the concave upward shape of the curve

from this point to pH 2.6 results from the steadily increasing quantity of activated complex. If the equilibrium constants for the interconversion of the several carbinol species were known, a much better idea of the manner in which the concentrations of these species vary with pH could be obtained by calculation. Unfortunately the constants are not known, and such calculations must be based upon estimated values for them. A number of calculations were carried out based on the assumption that the first and second acid ionization constants of malachite green carbinol are the same as those of p-phenylenediamine. While such an assumption is an approximation at best, it is probably not too bad in this case. (The constants for benzidine, which is more closely related structurally to malachite green carbinol would be preferable, but the experimental values do not appear to be as reliable as those for p-phenylenediamine.) From these data for the acid ionization constants<sup>(12)</sup> equilibrium expressions (10) and (11) are obtained. Equation (12) represents the equilibrium between the two forms of malachite green dye; the constant for this equilibrium has been determined experimentally<sup>(13)</sup>.



$$\frac{[H^+][H^+C]}{[H^+C^+H]} = 4.3 \times 10^{-3} \text{ m/l.} \quad (11)$$

$$\frac{[H^+][D]}{[H^+D]} = 7.4 \times 10^{-3} \text{ m/l.} \quad (12)$$

The concentrations of the various species of carbinol and dye calculated at several hydrogen ion concentrations from these equilibrium constants are summarized in Table 2.

Table 2

Relative Quantities of Various Species of Malachite Green Dye and Malachite Green Carbinol at Different Hydrogen Ion Concentrations

Conc. $H^+$ , m/l	Malachite Green Carbinol, % Species Present			Malachite Green Dye, % Species Present	
	<u>C</u>	<u>H<sup>+</sup>C</u>	<u>H<sup>+</sup>C<sup>+</sup>H</u>	<u>D</u>	<u>H<sup>+</sup>D</u>
	$10^{-5}$	76	24	0	100
$10^{-4}$	23	75	2	100	0
$10^{-3}$	3	79	18	99	1
$10^{-2}$	1	30	69	89	11
$10^{-1}$	0	4	96	23	77

It will be noticed that the change in concentration of the several species of carbinol with pH is in good agreement with

the qualitative description of these changes assumed to explain the effect of pH on the constant for the rate of approach to equilibrium.

Professor V. Schomaker has indicated to me in a private communication that it may be possible to obtain approximate relative values for the specific reaction rate constants for the conversion of each of the various carbinol species to malachite green dye. This procedure would involve first the determination of values for the constants  $k_1$  and  $k_2$ , which could be gotten from the values of  $k_1 + k_2$  obtained from the rate experiments described in the preceding pages and from values of  $K = k_1/k_2$  determined from additional experiments. The values of  $K$  could probably be analyzed for the ionization constants of the carbinol. From the pK values of the carbinol and dye species, together with certain assumptions about the corresponding values for the activated complex in relation to those of the dye and carbinol, the relative specific reaction rate constants might be obtained.

References to Part I

- (1) See, for example, Fieser and Fieser, "Organic Chemistry", Heath and Company, Boston, Mass., (1944) pp. 130-31.
- (2) H. Wieland, Ber., 54, 2353 (1921): *ibid.*, 55, 3639 (1922).
- (3) W. A. Waters, Trans. Faraday Soc., 42, 184 (1946).
- (4) Conant and Blatt, "Chemistry of Organic Compounds", third ed., McMillan Company, New York, (1947) pp. 532-33.
- (5) J. B. Conant and N. M. Bigelow, Jour. Am. Chem. Soc., 53, 676 (1931).
- (6) E. Fischer, O. Fischer, and O. Lehmann, Ber., 12, 798 (1879).
- (7) V. Villiger and E. Kopetschni, Ber., 46, 2916 (1912).
- (8) N. V. Sidgwick and T. S. Moore, J. Chem. Soc., 95, 889 (1909).
- (9) H. C. Biddle and C. W. Porter, *ibid.*, 37, 1571 (1915).
- (10) E. Q. Adams and L. Rosenstein, Jour. Am. Chem. Soc., 36, 1452 (1914).
- (11) H. C. Biddle, *ibid.*, 35, 273 (1913).
- (12) H. Scudder, "Conductivity and Ionization Constants of Organic Compounds", D. Van Nostrand Company, New York, (1914).
- (13) G. Schwarzenbach, H. Mohler, and J. Sorge, Helv. Chim. Acta, 21, 1636 (1938).

PART II

DETERMINATION OF SOME MOLECULAR STRUCTURES BY THE  
METHOD OF ELECTRON DIFFRACTION

- A. ADAMANTANE
- B. 1,3,5,7-CYCLOOCTATETRAENE



GENERAL INTRODUCTION

The procedure followed in these laboratories for the determination of a molecular structure by the diffraction of electrons has been discussed in detail in a number of theses and published articles. For this reason only a very brief summary of the method will be given here.

Electron diffraction photographs are prepared in the apparatus described by Brockway<sup>(1)</sup>. On these photographs one estimates visually<sup>(2)</sup> the distribution of intensity due to the structure of the molecule, and draws a "visual curve" to represent this intensity distribution. The visual curve is then compared with theoretical intensity curves calculated<sup>(3,4)</sup> for various models of the molecule by use of the equation<sup>(3)</sup>

$$I(q) = \frac{k}{\sum_i (Z_i - f)_i^2} \sum_{i,j} \frac{(Z_i - f)_i (Z_j - f)_j}{r_{ij}} e^{-2Z_i f^2} \sin\left(\frac{\pi}{10} q r_{ij}\right) \quad (13)$$

where  $Z_i$  = atomic number of atom  $i$

$F_i$  = atomic form factor for x-rays

$r_{ij}$  = distance between centers of atoms  $i$  and  $j$

$e^{-2Z_i f^2}$  = temperature factor

$q = 10s/\pi = (40/\lambda) \sin \phi / 2$

$\phi$  = angle of scattering

$\lambda$  = wave length of electrons, determined in a separate experiment by scattering from zinc oxide<sup>(6)</sup>. In most

cases it is possible to neglect the atomic form factor  $F$ , and equation (13) simplifies to (5)

$$I(q) = K' \sum_{i,j}' \frac{z_i z_j}{r_{ij}} e^{-2z_j q^2} \sin\left(\frac{\pi}{10} q r_{ij}\right) \quad (14)$$

Those models whose theoretical intensity curves are in agreement with the visual curve are satisfactory representations of the structure so far as the electron diffraction experiment is concerned. After suitable models have been found, the size of the molecule is determined by comparison of  $q$  values for the observed and the calculated maxima and minima. The limits of uncertainty in the structural parameters are determined by the limits of the range over which these parameters can be varied without giving a calculated intensity curve in disagreement with the visual curve.

Ordinarily the above procedure, called the "correlation procedure" is preceded by the calculation of a "radial distribution function" (5,3)

$$rD(r) = \sum_{q=1,2,\dots}^{q_{max.}} I(q) e^{-2q^2} \sin\left(\frac{\pi}{10} q r\right) \quad (15)$$

which is obtained from equation (14) by suitable mathematical manipulations. The radial distribution treatment leads

directly from the observed diffraction pattern to approximate values for the interatomic distances. These approximate values are then refined by the more sensitive correlation treatment.

## THE STRUCTURE OF ADAMANTANE

### Introduction

Electron diffraction investigations of the structure of hexamethylenetetramine<sup>(7,8)</sup> have led to a result for the bonded C-N distance which is about 0.04 Å. greater than the 1.44 Å. found for the same distance by x-ray studies of the crystal<sup>(9,10)</sup>. The crystal structure of adamantane (C<sub>10</sub>H<sub>16</sub>, see Figure 11), a molecule which has a configuration closely similar to that of hexamethylenetetramine, has been investigated by Nowacki<sup>(11)</sup> and by Giacomello and Illuminati<sup>(12)</sup>; and although a significant difference between the C-C bonded distance in the crystal and vapor of this substance would certainly not be expected, it seemed worthwhile to investigate this point by an electron diffraction determination of the structural parameters of the molecule.

### Experimental

Adamantane\* is a white, crystalline solid with an odor resembling that of camphor. Although its melting point is high, it sublimes easily and no trouble was experienced in the preparation of diffraction photographs when a high temperature nozzle<sup>(14)</sup> was used. Data on twelve maxima and shelves extending to  $q$  values of about 90 were obtained from the

---

\* The sample of adamantane used in this investigation was synthesized by Prelog and Seiwert<sup>(13)</sup>.

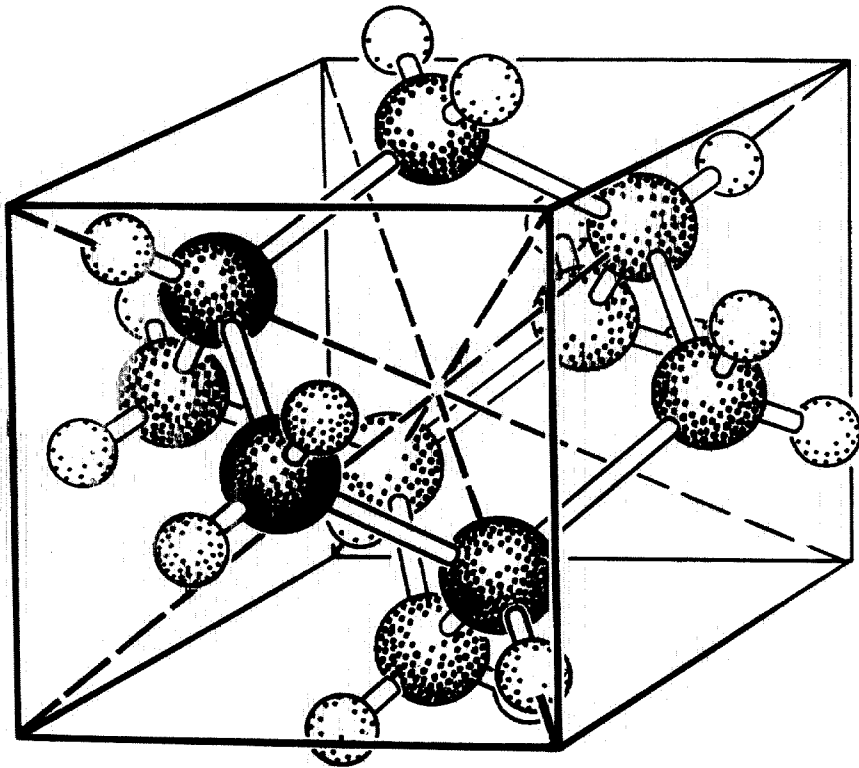


Figure 11

Adamantane

photographs. This is a somewhat smaller range of  $q$  values than was obtained by Schomaker and Shaffer for hexamethylenetetramine<sup>(8)</sup> and was occasioned by the short exposures necessary to preserve the very limited supply of material available. The camera distance was 11.05 cm. and the electron wave length 0.06085 Å. Corrections were made for expansion of the photographic film after exposure.

#### Radial Distribution Curve

The radial distribution curve (Figure 12) was calculated from equation (15) by use of punched cards<sup>(3,4)</sup>; the quantities  $I(q)$  were taken from the visual curve (Figure 12) drawn to represent the appearance of the photographs, and the constant  $a$  was chosen to give  $e^{-aq^2} = 1/10$  at  $q = 90$ . The resulting curve shows major peaks at 1.53 and 2.52 Å., which correspond to the bonded and to the shortest non-bonded C...C distances in a model with tetrahedral bond angles, such as C; in model C these distances are 1.540 and 2.515 Å. There are additional peaks at 1.00, 2.92, and 3.46 Å., and a broad feature at 2.20 Å. With the exception of the first none of these is sufficiently well resolved for a determination of interatomic distances, though they agree well with the final model shown by the vertical lines. The heavy lines denote the C...C distances and the light, the C...H; the lengths of the lines indicate the relative weights of the distances.

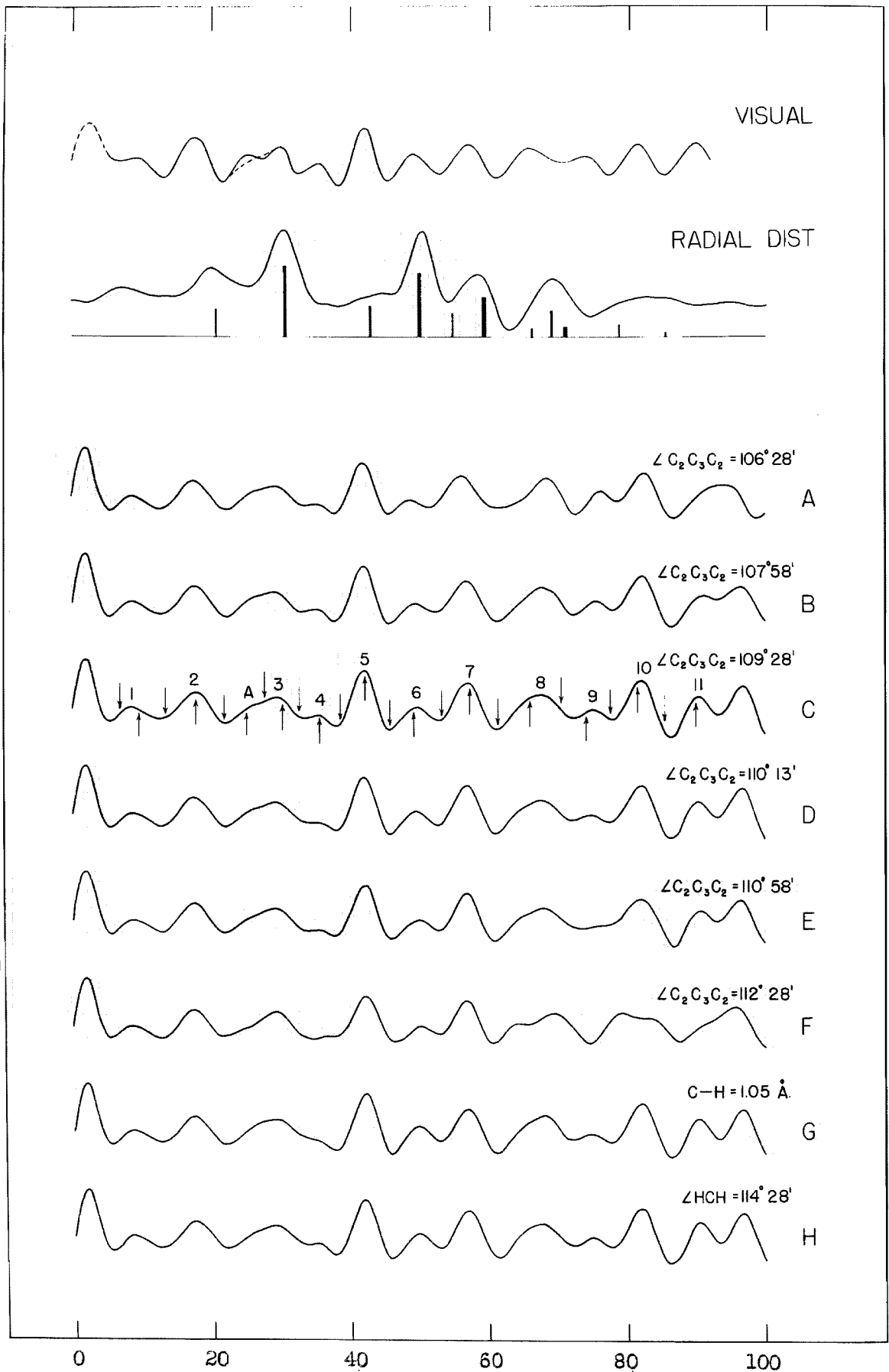


Figure 12. Theoretical Intensity Curves for Adamantane

The deviation of the peak at 1.00 Å. from the value 1.09 Å. normally obtained from bonded C···H interactions closely parallels the result obtained by Schomaker and Shaffer<sup>(8)</sup> in their study of hexamethylenetetramine.\*

#### Correlation of Visual and Intensity Curves

Intensity curves were calculated from equation (14) for a model of symmetry  $T_d - \bar{4}3m$  assuming C-C = 1.54 Å. throughout, C-H = 1.09 Å. except for model G, and  $\angle HCH = 109^\circ 28'$  except for model H. In models A to F the  $C_2C_3C_2$  bond angle is varied from  $106^\circ 28'$  to  $112^\circ 28'$ . Models G and H, which have tetrahedral C-C-C angles, are characterized by a shortened C-H distance (1.05 Å.) and an increased H-C-H angle ( $114^\circ 28'$ ), respectively. Terms representing all bonded and non-bonded atomic interactions except H···H were included in the calculations. An effective value of  $Z = 1.2$  was employed for hydrogen in order to approximate better its scattering power relative to carbon for small  $q$  values. The coefficient  $a_{ij}$  was given the value 0.00016 for bonded C-H, 0.00030 for all non-bonded C···H interactions\*\* and zero otherwise.

---

\* The visual curve for adamantane was drawn without previous knowledge of the appearance of the hexamethylenetetramine photographs or of the corresponding intensity curves, although subsequently the photographs of the two substances were carefully compared and found to be closely similar. The errors in the two visual curves which correspond to the errors at 1.0 Å. in the two radial distribution functions are thus evidently nearly alike. Perhaps this is because they represent errors of interpretation which are in some way peculiar to the types of features shown by hexamethylenetetramine and adamantane.

\*\*The value 0.00030 is frequently used for C···H interactions through one bond angle, but it is felt to be a reasonable one for all non-bonded C···H interactions here because of the relative rigidity of the carbon skeleton of adamantane.



Comparison of the calculated curves with the visual curve shows model A to be unacceptable; minimum 8 appears in the calculated curve as far too broad and the relative depths of minima 9 and 10 are inverted. Curve B is somewhat better than A, but the disagreement in the relative depths of minima 9 and 10 is still present. Curve C is generally satisfactory\*. Curve D is acceptable although maximum 4 is a poorer representation of the photographs than the same maximum in C. Curves G and H are both acceptable although G is not as satisfactory as C in the region of maximum 4.

---

\* The main aspects of disagreement in the correlation of model C, which is the best model, with the observed intensity distribution are seen to involve (1) the relative depths of minima 1 and 2, (2) the strength of shelf A, (3) the shape of maximum 8, and (4) the relative depths of minima 5 and 6. The first two items do not appear to be serious; estimates of the depth of the first minimum are subject to considerable error, and a re-examination of the photographs indicates the exaggeration of shelf A to be a simple misinterpretation (the dotted line is felt to be a more accurate representation of this feature). Item (3) also arises from errors of interpretation, as shown by comparing photographs of adamantane and hexamethylenetetramine; the appearance of maximum 8 is closely similar and was satisfactorily represented by Schomaker and Shaffer<sup>(8)</sup> in their visual intensity curve for hexamethylenetetramine. It is difficult to explain the reversal of minima 5 and 6 (item (4)). Perhaps the trouble is due to a tendency to compensate incorrectly for the background intensity, which is difficult to estimate in patterns as complicated as that of adamantane.

### Conclusions

A comparison of the observed  $q$  values with those calculated for model C (Table 3), a consideration of the radial distribution functions, and comparisons of visual and calculated curves lead to the following conclusions regarding the structure of the adamantane molecule: symmetry  $T_d - \bar{4}3m$  (assumed),  $\angle HCH = 109^{\circ}28'$  (assumed),  $C-H = 1.09 \text{ \AA.}$  (assumed)  $C-C = 1.54 \pm 0.01 \text{ \AA.}$ ,  $\angle C_2C_3C_2 = 109.5 \pm 1.5^{\circ}$ . The upper limit of the  $\angle C_2C_3C_2$  determination is especially conservative. These results are in agreement with those found in x-ray diffraction studies of the crystal. No attempt was made to establish the limits of uncertainty in the  $\angle HCH$  and the  $C-H/C-C$  parameters, but it is certain that such a determination cannot be made to within sizeable limits of error. There is no doubt, however, that the assumed values for these parameters are sufficiently accurate so that their uncertainty induces no additional uncertainty in the values obtained for  $C-C$  and  $\angle C_2-C_3-C_2$ .

Table 3

ELECTRON DIFFRACTION DATA FOR ADAMANTANE

Max.	Min.	q <sub>obs.</sub>	q <sub>calc.</sub> (Model C)	q <sub>calc.</sub> /q <sub>obs.</sub> *
	1	6.5	5.3	(0.815)
1		9.6	8.5	(0.885)
	2	13.3	12.6	(0.947)
2		17.8	17.8	1.000
	A	21.9	22.2	1.014
A		25.1	25.5	(1.016)
	3	27.8	27.2	(0.978)
3		30.3	29.3	(0.967)
	4	32.8	33.7	1.027
4		35.7	35.3	0.989
	5	38.7	38.1	0.984
5		42.2	42.0	0.995
	6	45.8	46.2	1.009
6		49.3	49.8	1.010
	7	53.3	53.2	0.998
7		57.4	57.0	0.993
	8	61.4	61.2	0.997
8		66.0	67.3	(1.020)
	9	70.6	72.3	1.024
9		74.2	75.2	1.013
	10	77.7	78.1	1.005
10		81.7	82.2	1.006
	11	85.5	86.7	1.014
11		90.1	90.5	1.004
		Average		1.004
		Average deviation		0.008

\* Parenthesized values were omitted in evaluation of averages, bracketted values were given half weight.

## THE STRUCTURE OF 1,3,5,7-CYCLOÖCTATETRAENE

### Introduction

The structure of cycloöctatetraene is of great theoretical importance to chemists because of the unique relationship between this molecule and the benzene molecule, a relationship which suggests the possibility of a comparable resonance stabilization and, hence, of aromatic character. Although the chemistry of cycloöctatetraene<sup>(15)</sup> is not that of an aromatic compound, the results recorded by different investigators working on its physical-chemical character<sup>(16-20)</sup> have led to considerable confusion in this regard. For example, data from an x-ray diffraction investigation currently in progress<sup>(16)</sup> indicate cycloöctatetraene to have two different C-C bonded distances and to possess the molecular symmetry  $D_{2d}$ ; this result is in complete disagreement with the result from an earlier electron diffraction study of the vapor<sup>(17)</sup> from which it was concluded that all bonded C-C distances are equivalent and the molecule has symmetry  $D_{4d}$ .

The general confusion regarding the structure of cycloöctatetraene, particularly that arising from the disagreement between the results of the x-ray and electron diffraction determinations, and the importance of the structure have led to the present study. This investigation shows that cycloöctatetraene has two C-C bonded distances, which are about

equal to the normal double bond distance and to the conjugated single bond distance, and a C-C-C bond angle of about  $126\frac{1}{2}^{\circ}$ . The molecule has the symmetry  $D_{2d}$  in agreement with the result from x-ray diffraction.

### Experimental

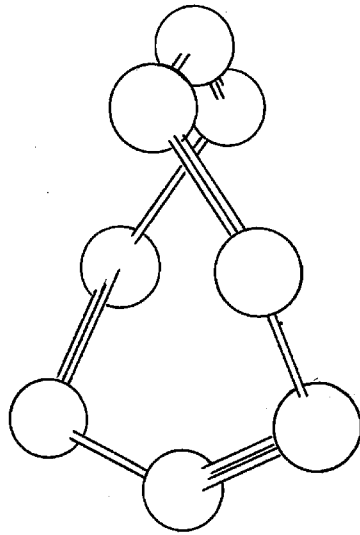
The sample of cycloöctatetraene used in this investigation was kindly furnished by Professor R. C. Lord of the Massachusetts Institute of Technology. It contained a small amount (less than 3%) of styrene, which was taken into account in the calculations of theoretical intensity curves. The photographs were made in the apparatus described by Brockway<sup>(1)</sup> with a camera distance of 10.93 cm. and an electron wave length of  $0.06061 \overset{\circ}{\text{Å}}$ . Corrections were made for film expansion.

### Radial Distribution Curve

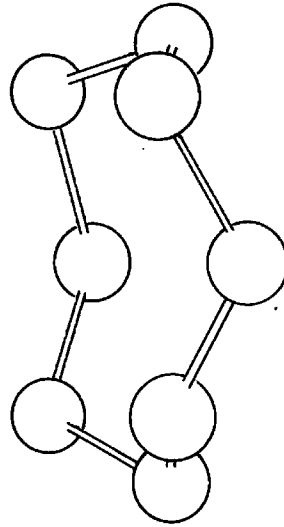
The radial distribution function\* (Figure 14) was evaluated by punched card summation of equation (15); the values of  $I(q)$  were taken from the visual curve (Figures 16, 17) and

---

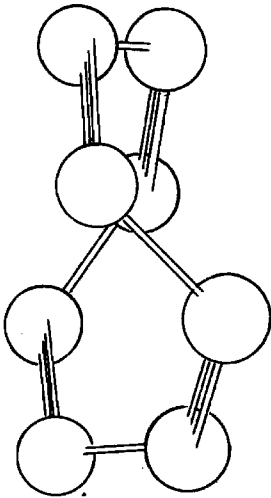
\* It is important to emphasize that the earlier stages of the interpretation of the electron diffraction photographs of cycloöctatetraene (through the drawing of visual curves and the evaluation of the radial distribution functions) were carried through by both Professor V. Schomaker and myself working completely independently. The results obtained by us were in substantial agreement on all points. The only difference worthy of mention involved the position of the first main peak in the radial distribution curves; in Professor Schomaker's curve this peak appeared at about  $1.40(5) \overset{\circ}{\text{Å}}$ , and in mine (Figure 14) at about  $1.38 \overset{\circ}{\text{Å}}$ . We have not yet determined the reason for this difference, but it is not in any way obvious from the appearance of the two visual curves.



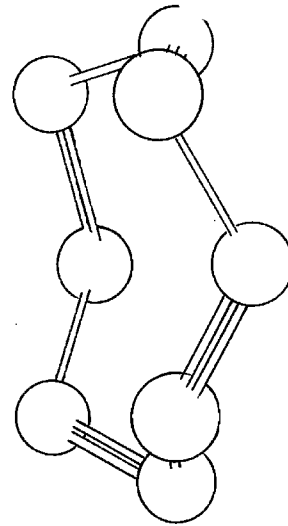
$S_4$



$D_{4d}$



$D_{2d}$  "TUB"



$D_4$

Figure 13. Cyclooctatetraene. Models of various molecular symmetries investigated.

$a$  was so chosen as to make  $e^{-aq^2} = 1/10$  at  $q = 100$ . The radial distribution curve has main peaks at 2.48 and 1.38 Å. and a broad feature at approximately 3.20 Å. The first of these peaks has a half-width which corresponds closely to that expected from a single interatomic distance; it represents C-C interactions through one bond angle. The peak at 1.38 Å. is notably broad and is a representation of unresolved singly bonded and doubly bonded C-C distances. If these distances are taken as 1.33 and 1.44 Å., respectively, the C-C-C bond angle is calculated to be about  $127^\circ$ . The broad feature at 3.20 Å. arises from a number of longer interatomic distances which lie too close together to be resolved.\*

The radial distribution function for cyclooctatetraene is particularly useful because the several symmetries which have been proposed for this molecule lead to quite different longer C-C interactions. Although these longer interatomic distances are not resolved in the calculated curve, the only slightly unsymmetrical appearance of the peak which represents them suggests that they are distributed in a more or less regular fashion on either side of the "center of gravity", that is, on either side of a point at about 3.20 Å. In Figure 14 all the C-C interatomic distances are shown as

---

\* Although these distances are too close together to be resolved in the radial distribution function with its low weighting of the data for higher angles of scattering, they are not necessarily too close together to be resolved by the more sensitive correlation procedure.

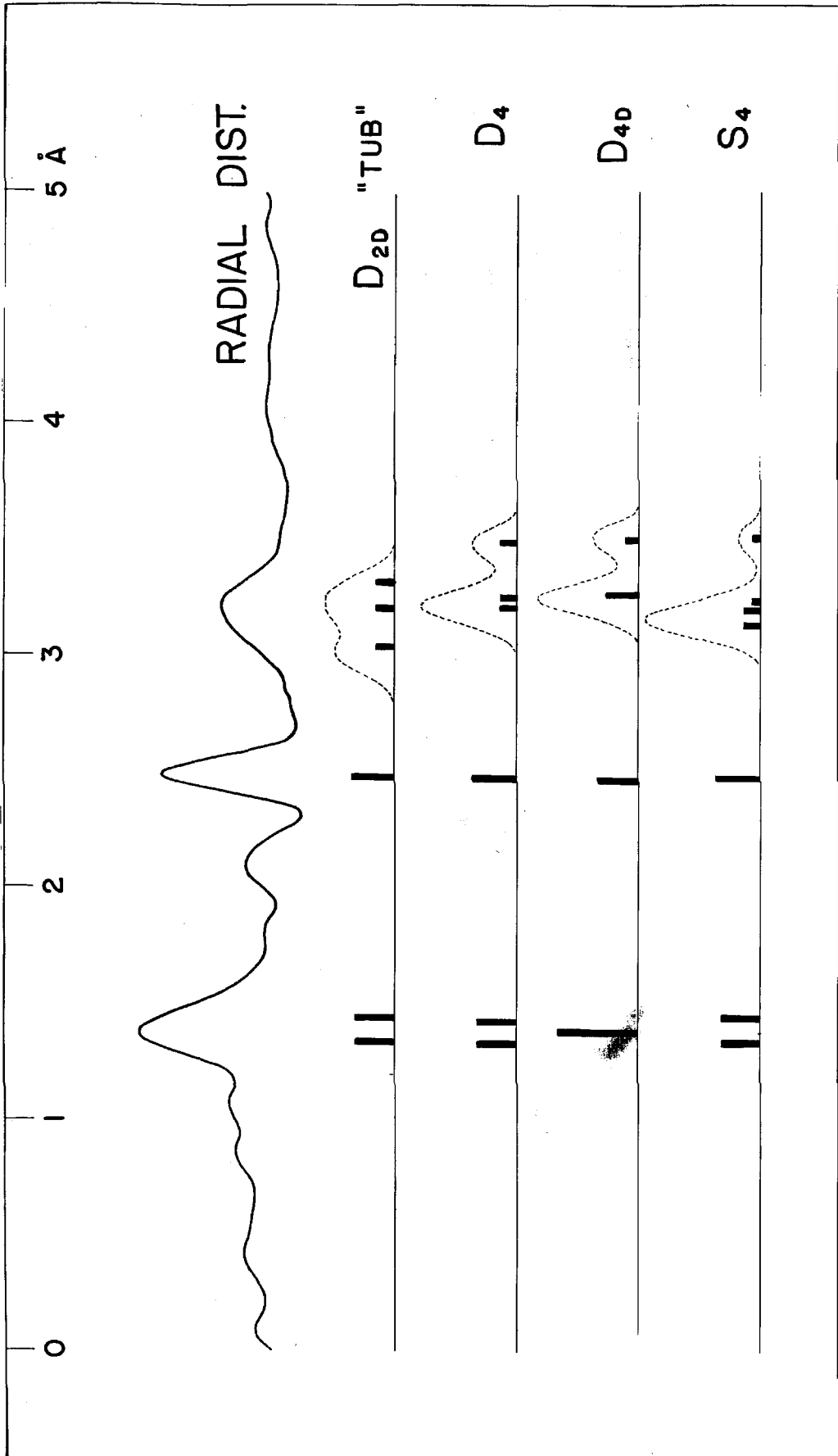


Figure 14. Cyclooctatetraene. Radial Distribution Curve.



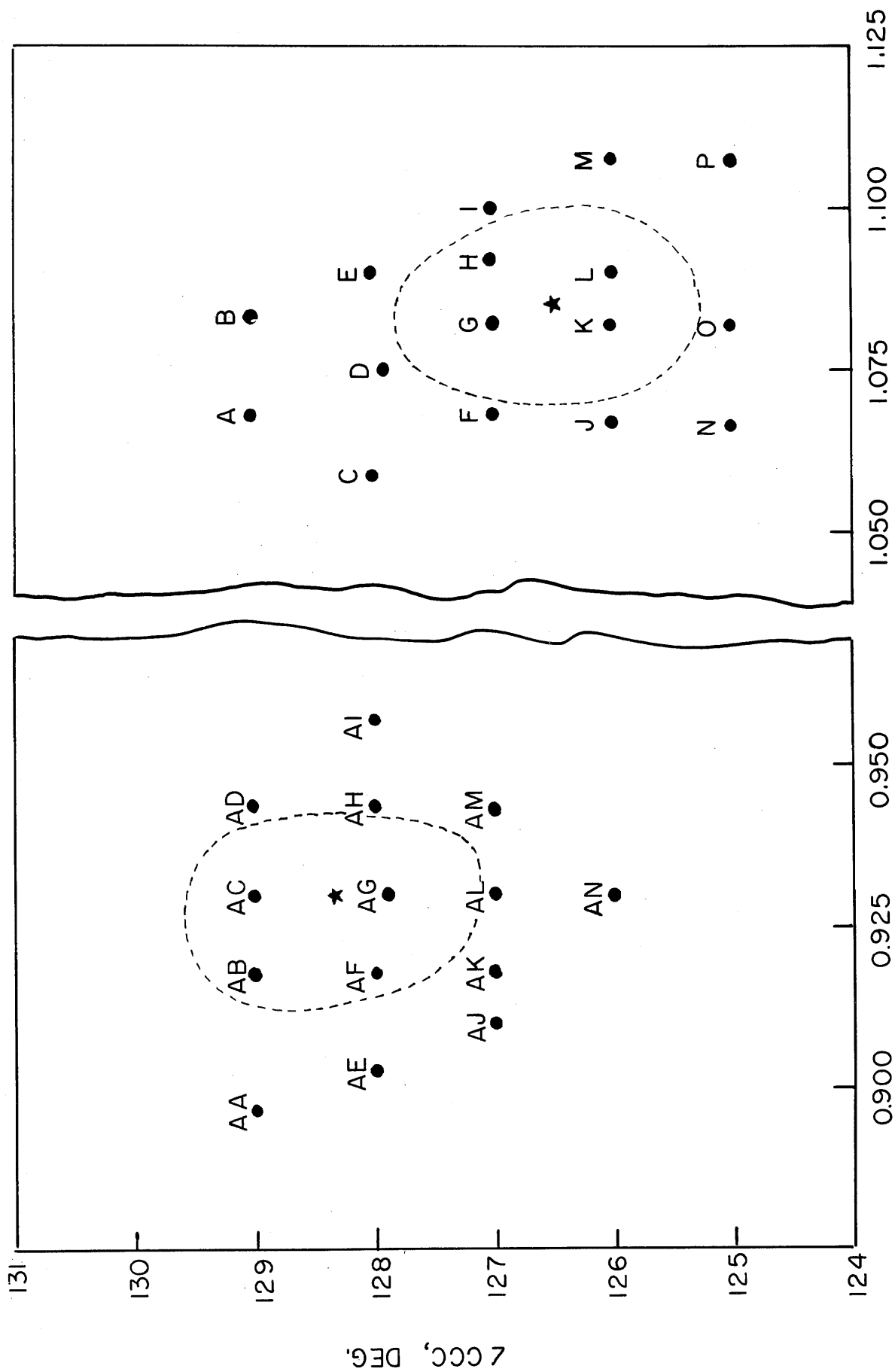
vertical lines for models of symmetries  $D_{2d}$  "tub",  $D_4$ ,  $D_{4d}$ , and  $S_4$  (models of these symmetries are shown in Figure 13) calculated from reasonable values of the C-C bonded distances and C-C-C bond angle; the heights of the lines are proportional to the weights ( $n Z_i Z_j / r_{ij}$ ) of the distances and the dotted curves represent the shape of an idealized radial distribution function in the region of these interactions\*. It is apparent that the  $D_{2d}$  "tub" model provides the best, and, in general, an excellent fit to the radial distribution curve, followed in decreasing order by the models of  $D_4$ ,  $S_4$ , and  $D_{4d}$  symmetry.

#### Theoretical Intensity Curves

Several theoretical intensity curves were calculated for each of the molecular symmetries  $D_{4d}$ ,  $D_4$ , and  $S_4$ , and a considerably larger number for the  $D_{2d}$  "tub" using Equation (14). The first  $D_{4d}$  curve and the curves for the  $D_4$  and  $S_4$  symmetries shown in Figure 16 were calculated from best values of the bonded C-C distances and C-C-C bond angle as

---

\* In a calculation of our radial distribution function a Fourier component of the visual intensity curve corresponding to an interaction between two point atoms at a definite distance gives rise to a peak having approximately the form of a Gaussian error curve; the half width of these peaks is dependent upon the coefficient  $a$  in the convergence factor  $e^{-aq^2}$ . The appearance of a feature in the radial distribution curve resulting from several unresolved interatomic distances may, then, be approximated by adding together a number of Gaussian curves of the proper half widths and of heights proportional to the weights of the distances.



INCLINED BOND DISTANCE  
HORIZONTAL BOND DISTANCE

Figure 15. Cyclooctatetraene. Parameters for D<sub>2d</sub> "tub" Models.

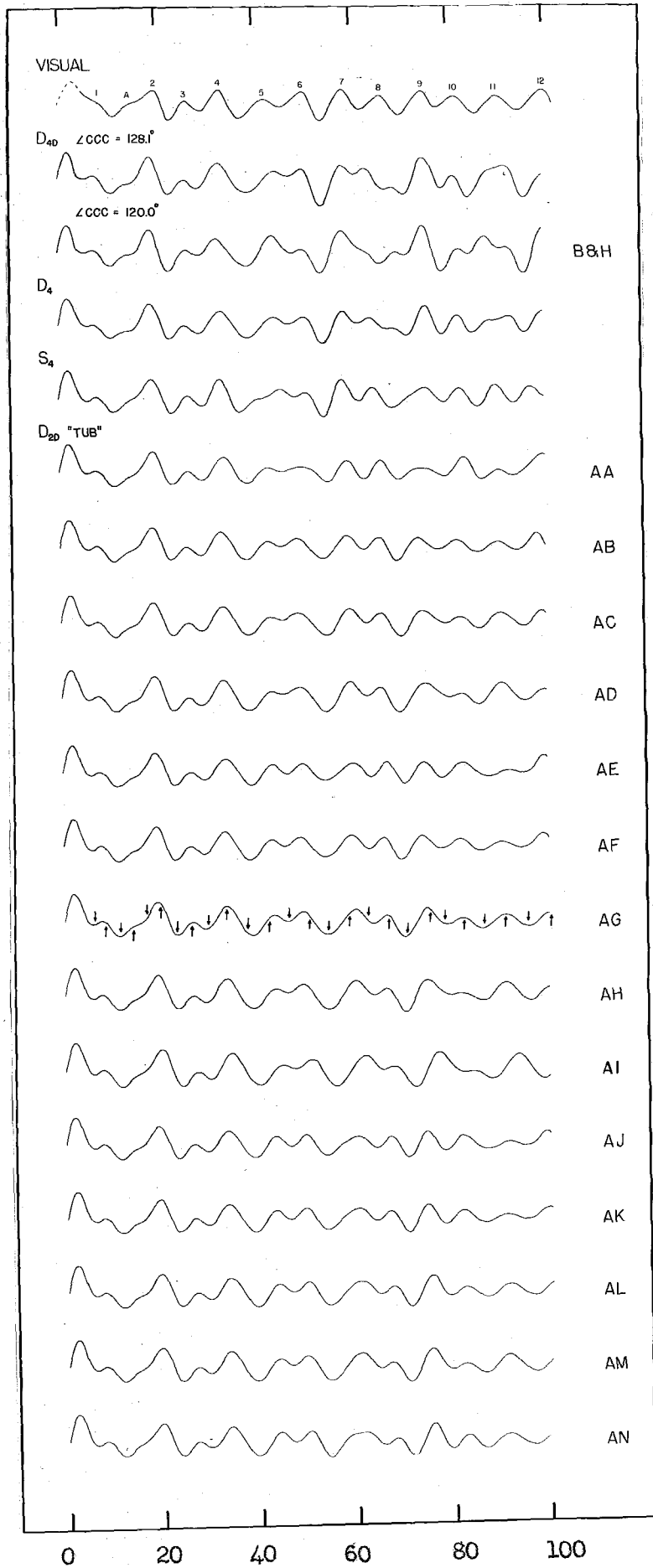


Figure 16. Theoretical Intensity Curves for Cyclooctatetraene.

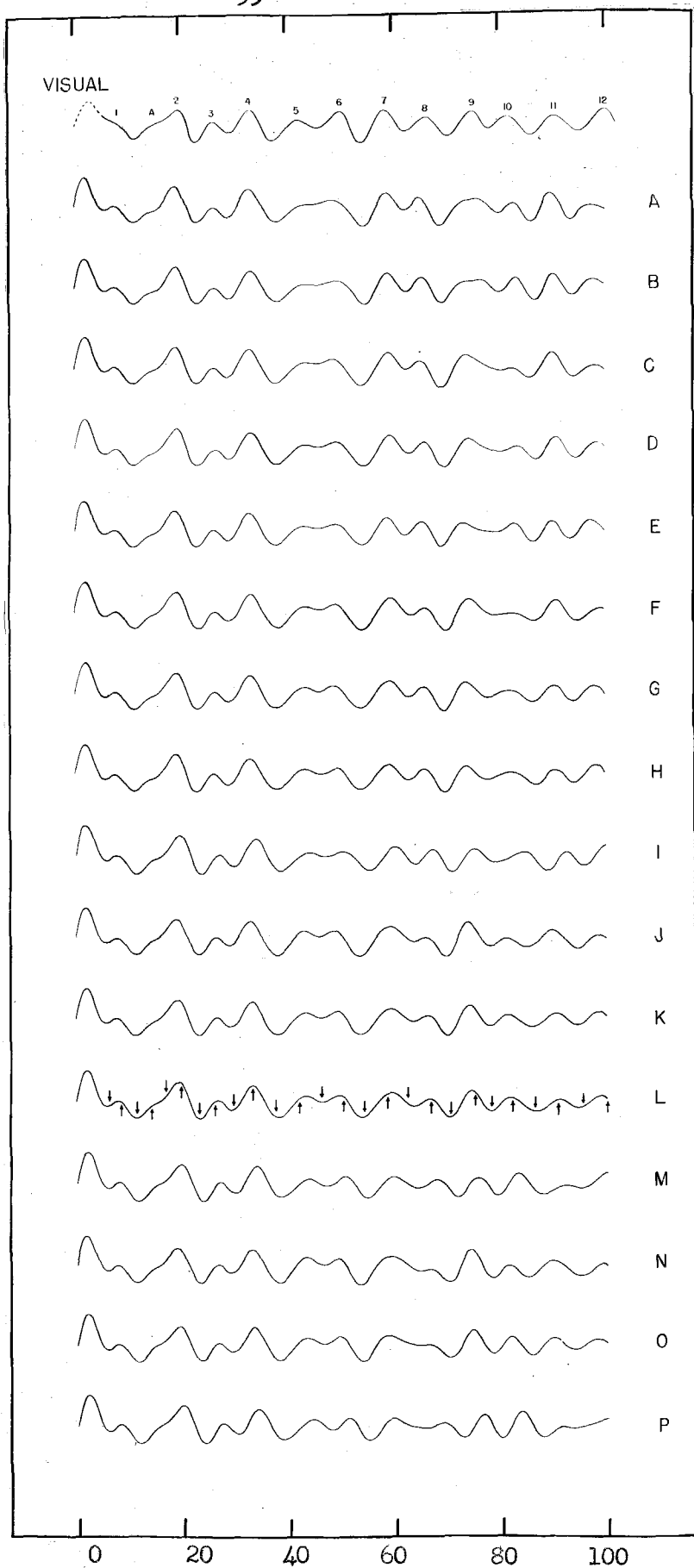


Figure 17. Theoretical Intensity Curves for Cyclooctatetraene.

determined from the radial distribution curve; these are the same models used in Figure 14. For  $D_{4d}$  these parameters are 1.38 Å. and  $128^\circ$ ; for  $D_4$ , 1.33 Å., 1.43 Å., and  $127^\circ$ , and for  $S_4$ , 1.34 Å., and  $127^\circ$ . Curves for symmetry  $D_{2d}$  "tub" are presented in Figures 16 and 17 for models in which the  $\angle CCC$  was varied from  $125^\circ$  to  $130^\circ$  and the ratio of the inclined C-C bond distance to the horizontal C-C bond distance from 0.897 to 1.108. The average of these distances was kept at  $1.38 \pm 0.025$  Å. except in the case of model AI, where it was 1.34 Å. Figure 15 shows the values of these parameters for each  $D_{2d}$  "tub" model. For each theoretical curve shown terms were included to represent all  $C \cdots C$  interactions, bonded C-H distances (assumed 1.09 Å.), and  $C \cdots H$  interactions through one bond angle ( $\angle C=C-H = \angle CCC$  assumed). The value of the coefficient  $a_{ij}$  for these terms was taken as 0, 0.00016, and 0.00030, respectively.

#### Correlation of Visual and Calculated Intensity Curves

A comparison of the visual curve with the curves calculated for models of molecular symmetries  $D_{4d}$ ,  $D_4$ , and  $S_4$  shows in each of these cases a number of disagreements so serious as to eliminate the model completely. In the first  $D_{4d}$  curve this occurs in the region of maxima 7, 8, and 9, and again at maximum 11. Model B&H, the preferred model of Bastianson and Hassel, is even less desirable; in addition

to those difficulties the relative heights of maxima 5 and 6 are strongly reversed. For the  $D_4$  curve the disagreements are similar regions and are not significantly improved over the  $D_{4d}$ . The model of symmetry  $S_4$  is unacceptable because of the appearance of maxima 5 and 6; maximum 5 has a shoulder of such prominence as to give of the whole an appearance approaching that of a triplet. It is important to emphasize here that several other curves (not shown) have been calculated for both the  $D_4$  and  $S_4$  symmetries, and that no acceptable fit to the visual curve is found\*; indeed, none of these curves is significantly better than those described above.

In marked contrast to the symmetries discussed above, curves calculated for  $D_{2d}$  "tub" models are found to be in very close agreement with the visual curve in two quite different regions of parameter combinations. These are shown in Figure 15 enclosed by the dotted lines, which represent the limits of uncertainty. These regions differ primarily in the ratio of the inclined bonded distances to the horizontal bonded distances, which, of course, means the position of the double bonds and single bonds.

In considering those models having a ratio of inclined bond distance to horizontal bond distance less than one, it

---

\* The parameter ranges covered are as follows:  $D_4$ ,  $\angle CCC = 127-129^\circ$ ,  $C=C/C-C = 1.060-1.090$ ;  $S_4$ ,  $\angle CCC = 125-129^\circ$ ,  $C=C/C-C = 1.064-1.100$ .

is obvious that AG is generally satisfactory, AC only a little less so, and AA, AE, AJ, AN, and AI generally bad. Models AD and AH give a poor representation of the height of the tenth maximum relative to the ninth and the eleventh, and, especially in the case of AD, show a broadness of the ninth maximum considerably out of proportion in comparison with the eighth. Curves AK, AL, and AM suffer from a common defect, namely, the broad, rounded character of the seventh maximum. Although this characteristic improves substantially in going from AK to AM, the increasing height of the seventh, ninth and eleventh maxima relative to the eighth and tenth maintains the generally poor fit. Model AB shows maximum eight as too strong relative to adjacent maxima, a difficulty slightly improved by AF but offset by the poorer representation of the shape of the seventh minimum. Curve AG is the most satisfactory of those shown, but it seems apparent that the best model has a slightly greater bond angle (about  $128\frac{1}{3}^\circ$ ) and about the same bond ratio, corresponding to a point about  $\frac{1}{3}$  of the way along a line from AG to AC in Figure 15. An intensity curve for such a model should provide a better representation of the ninth maximum relative to those near it without altering too greatly the more desirable characteristics of curve AC in the region of the fifth, sixth, seventh, and eighth maxima and minima, and the ninth minimum.

Of those  $D_{2d}$  models having a ratio of inclined to horizontal bond distance greater than one, A,B,C,D,E,N,O, and P are generally poor, G,H,K, and L satisfactory, and F,I,J, and M, models which lie close to the limits of uncertainty. Models F and M are unsatisfactory at the tenth maximum, as is model J, which in addition shows the ninth maximum as too high in comparison with the sixth and seventh. Curve I shows maxima 5 and 6 as not strong enough relative to those on either side, and maximum 8 as too strong. Of the acceptable curves, K and L represent the shape of the seventh maximum and its height relative to the ninth somewhat more poorly than do G and H, which in turn are less satisfactory at the tenth maximum\*. These considerations suggest that the best

---

\* The acceptable curves also show three minor disagreements with the visual curve. These are (1) the appearance of the first maximum, (2) the depth of the seventh minimum relative to the fifth and ninth, and (3) the relative heights of the fifth and sixth maxima, (items (1) and (2) are peculiar to acceptable curves in both regions of acceptability). The first item is of no importance, it is very difficult to estimate the shape of the first maximum because of the intense background at this point on the photograph. Item (2) is likewise considered to be little importance. It probably arises from the considerably greater broadness of this minimum as compared with others of comparable depth near it, and from the difficulty of making comparisons across the adjacent asymmetric features. Item (3) probably arises from errors of interpretation brought about by a tendency to over-compensate for the background intensity. We have carefully reexamined the photographs in this region, and we believe from considerations based upon the appearance of the height of the third maximum relative to the fourth that the fifth maximum should properly have been drawn higher relative to the sixth.



interpolated model lies approximately at the intersection of lines drawn from G to L and from H. to K in Figure 15; such a model has a bond angle of about  $126\frac{1}{2}^{\circ}$  and a bond ratio of about 1.085, and would be in good agreement with all the features of the diffraction pattern so far as they can be interpreted.

Electronic Structure of Cycloöctatetraene  
and Choice of a Best Model

Although the cycloöctatetraene molecule has been found to possess the symmetry  $D_{2d}$  "tub", it is apparent that the problem of its electronic structure has not been settled by the electron diffraction experiments. The qualitative comparisons described in the preceding section and the values of  $q_{\text{calc}}/q_{\text{obs}}$  given in Table 4 indicate clearly that electron diffraction data extending only to  $q$  values of about 100 ( $s \sim 31.5$ ) do not permit a choice between a configuration with the double bonds in the horizontal positions, as shown in Figure 13, or one with the double bonds in the inclined positions. It is certainly more likely, however, that the former of these two alternatives represents the actual case. The normal strain-free configuration of the group  $C-C=C-C$  is coplanar with a  $C-C=C$  bond angle of about  $125^{\circ}$ . These conditions are closely approximated by the best interpolated model having double bonds in the horizontal positions ( $C-C=C-C$  coplanar,  $\angle C-C=C = 126\frac{1}{2}^{\circ}$ ), whereas the

best interpolated model of the other configuration has a slightly larger C-C-C bond angle ( $128-1/3^\circ$ ) and a non-coplanarity of the C=C-C group amounting to a rotation of approximately  $38^\circ$  about the double bond. These considerations indicate the correct structure for cyclooctatetraene to be one having the molecular symmetry  $D_{2d}$  with alternate double and single bonds, and with double bonds located in the horizontal positions.\*

The structural parameters\*\* for the best model are: C-C =  $1.435 \pm 0.030$ , C=C =  $1.326 \pm 0.016$  Å.,  $\angle$  CCC =  $126.5 \pm 1.5$ ,  $\angle$  CCH =  $126.5 \pm 1.5$  (assumed), C-H = 1.09 Å. (assumed).

These structural parameters for cyclooctatetraene, a normal C-C bond distance, a C-C single bond distance about equal to that found in conjugated polyenes, and a C=C-C bond angle approximately equal to  $125^\circ$ , are in complete accord with its aliphatic, highly unsaturated character, and with the small resonance energy as calculated from recent

---

\* Experimental evidence which lends support to this choice of the position of the double bonds was obtained by an electron diffraction investigation of tetraphenylene (1,2,3,4,5,6,7,8-tetrabenz- $\Delta^{1,3,5,7}$ -cyclooctatetraene), I. L. Karle and L. O. Brockway, Jour. Am. Chem. Soc., 66, 1974 (1944). Satisfactory agreement was obtained between the observed pattern and theoretical intensity curves calculated for models which may be considered as derived from a cyclooctatetraene with double bonds in the horizontal positions.

\*\* The establishment of limits of error for the bonded C-C distances is obtained from calculations based upon the size of the region of acceptability shown in the right side of Figure 10 and upon values of  $q_{calc}/q_{obs}$  shown in Table 4.

thermochemical measurements\*. Several investigations of the Raman and infra-red spectrum of cyclooctatetraene have been carried out(17,18,19) and, although different interpretations of the data have led to proposals of several molecular symmetries, the data themselves are consistent and do not appear to be in disagreement with the above model.

---

\* E. J. Prosen, W. B. Johnson, and F. D. Rossini, Jour. Am. Chem. Soc., 69, 2068 (1947). An earlier report (See B.I.O.S. report N-137 Item 22 (1945)) of the heat of combustion, which gives a calculated resonance energy of 25.4 kcal./mole, cannot be considered in agreement with the structural results. This value is only slightly less per C-H group than one-half that found for benzene, and is undoubtedly incorrect.

Table 4

Comparison of Calculated and Observed Positions of Maxima and Minima

Min. Max.	$q_{\text{obs}}$	AG	AC	$\frac{2AG + AC}{3}$	L	K	G	H	$\frac{L + K + G + H}{4}$
1	6.3	(0.936)	(0.921)	(0.931)	(0.952)	(0.952)	(0.952)	(0.937)	(0.948)
1	8.5	(0.918)	(0.906)	(0.914)	(0.941)	(0.918)	(0.918)	(0.918)	(0.924)
A	11.6	(0.974)	(0.974)	(0.974)	(0.914)	(0.991)	(0.974)	(0.983)	(0.965)
A	14.4	(0.972)	(0.944)	(0.963)	(0.993)	(1.014)	(0.972)	(0.972)	(0.988)
2	17.0	(0.994)	(0.924)	(0.971)	(0.970)	(0.941)	(0.941)	(0.918)	(0.942)
2	19.9	0.965	0.960	0.963	0.970	0.970	0.965	0.965	0.968
3	23.3	1.000	1.004	1.002	1.013	1.008	1.004	1.000	1.006
3	26.3	1.008	0.992	1.003	1.027	1.015	1.008	1.004	1.014
4	29.7	0.980	0.976	0.978	0.993	0.990	0.983	0.986	0.987
4	33.4	1.000	1.000	1.000	1.003	1.000	0.991	0.994	0.997
5	37.7	1.029	1.021	1.026	1.016	1.011	1.013	1.016	1.014
5	42.1	1.024	1.021	1.023	1.033	1.033	1.028	1.033	1.032
6	46.3	0.991	0.983	0.988	1.004	1.002	0.994	1.002	1.000
6	50.5	0.970	0.964	0.968	0.982	0.974	0.968	0.978	0.975
7	54.4	0.996	1.002	0.998	0.993	0.989	0.993	0.994	0.992
7	58.6	1.022	1.012	1.018	1.015	1.014	1.008	1.010	1.012

Table 4 (continued)

Min. Max. $q_{Obs}$	AG	AC	<u>2AG <math>\rightarrow</math> AC</u>			L	K	G	H	<u>L <math>\rightarrow</math> K <math>\rightarrow</math> G <math>\rightarrow</math> H</u>			
			3							4			
8	62.5	1.016	1.006	1.013	1.021	1.019	1.006	1.008	1.014				
8	66.8	0.993	0.985	0.990	1.000	0.992	0.985	0.988	0.991				
9	70.6	0.994	0.986	0.991	1.000	0.994	0.987	0.992	0.994				
9	75.2	0.991	0.988	0.990	0.992	0.987	0.981	0.984	0.996				
10	78.1	1.008	1.012	1.010	1.001	1.001	0.992	0.999	0.999				
10	82.2	0.996	0.999	0.997	0.998	0.993	0.996	1.004	0.998				
11	86.5	0.994	0.994	0.994	1.000	0.995	0.999	1.007	1.000				
11	90.8	1.002	0.997	1.000	1.002	0.999	0.994	1.000	0.999				
12	95.4	1.004	0.999	1.002	0.995	0.994	0.985	0.988	0.991				
12	100.1	(0.997)	(0.989)	(0.994)	(0.985)	(0.985)	(0.977)	(0.982)	(0.982)				
Av., 20 features	0.999	0.995	0.998	1.003	0.999	0.994	0.998	0.998	0.999				
Av., deviation	0.012	0.013	0.012	0.010	0.011	0.011	0.011	0.010	0.010				
Av., 13 features	0.999	0.996	0.998	1.000	0.996	0.992	0.992	0.996	0.997				
Av., deviation	0.010	0.011	0.010	0.008	0.008	0.008	0.008	0.008	0.007				

(2) averages taken with omission of the unsymmetrical third and fourth minima, and the third, fifth, sixth, seventh and eighth maxima.

References to Part II

- (1) L. O. Brockway, Rev. Modern Phys., 8, 231 (1936).
- (2) L. Pauling and L. O. Brockway, J. Chem. Phys., 2, 867 (1934)
- (3) P. A. Shaffer, Jr., V. Schomaker, and L. Pauling, Jour. Chem. Phys., 14, 659 (1946).
- (4) P. A. Shaffer, Jr., V. Schomaker, and L. Pauling, *ibid.*, 14, 648 (1946).
- (5) R. Spurr and V. Schomaker, *ibid.*, 64, 2693 (1942).
- (6) C. S. Lu and E. W. Malmberg, Rev. Sci. Instr., 14, 271 (1943). Wave lengths are determined in kx units and converted to Angstrom units.
- (7) G. C. Hampson and A. J. Stosick, Jour. Am. Chem. Soc., 60, 1814 (1938).
- (8) V. Schomaker and P. A. Shaffer, Jr., *ibid.*, 69, 1555 (1947).
- (9) R. G. Dickinson and A. L. Raymond, *ibid.*, 45, 22 (1923).
- (10) R. Brill, H. Grimm, C. Hermann, and A. Peters, Ann. Physik, 34, 393 (1939).
- (11) W. Nowacki, Helv. Chim. Acta, 28, 1233 (1945).
- (12) G. Giacomello and G. Illuminati, Ricerca Sci., 15, 559 (1945).
- (13) V. Prelog and R. Seiwert, Ber., 74, 1644, 1769 (1941).
- (14) L. O. Brockway and K. J. Palmer, Jour. Am. Chem. Soc., 59, 2181 (1947).
- (15) See, for example, A. W. Johnson, Sci. Progress, 35, 506 (1947).
- (16) H. S. Kaufman, I. Frankuchan, and H. Mark, Abstract No. 6 Division of Physical and Inorganic Chemistry, American Chemical Society Meeting, New York, Sept. 15, 1947.
- (17) O. Bastiansen and O. Hassel, Tids, Kjemi, Bergvesen Met., 7, 55 (1947). See also O. Bastiansen, O. Hassel, and A. Langseth, Nature, 160, 128 (1947).

- (18) E. R. Lippincott and R. C. Lord, Jr., Jour. Am. Chem. Soc., 68, 1868 (1946).
- (19) N. C. Flett, W. T. Cave, E. E. Vago, and H. W. Johnson, Nature, 159, 739 (1947).
- (20) R. C. Pink and A. R. Ubbelohde, Nature, 160, 502 (1947).

PART III

THE MOLECULAR STRUCTURE OF ARSENOBENZENE. DETERMINATION  
OF THE UNIT CELL AND SPACE GROUP OF THE CRYSTAL

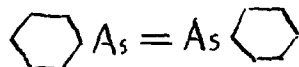


THE MOLECULAR STRUCTURE OF ARSENOBENZENE. DETERMINATION  
OF THE UNIT CELL AND SPACE GROUP OF THE CRYSTAL

Introduction

The work described in this section was carried out jointly by Dr. Jürg Waser and myself. We are indebted to Professor L. Pauling for the suggestions which led to the investigation.

Although arsenobenzene has been known since 1881 when it was synthesized by Michaelis and Schults<sup>(1)</sup> its molecular formula is still uncertain. Chemists ordinarily consider the formula to be  $(C_6H_5-As)_2$ , which is written in structural form with the two arsenic atoms doubly bonded to each other.



Determinations of the molecular weight of this substance have been made by several investigators<sup>(2,3,4)</sup> in a number of different solvents using both ebulloscopic and cryoscopic methods (Table 5). The determinations, however, do not lead to values in agreement with the above formula, but indicate a degree of association which varies from 2 to 6 monomer units (Monomer unit =  $\text{C}_6\text{H}_5\text{As}$  ) per molecule depending upon the solvent. In one case considerably different molecular weights were obtained by different investigators using the same solvent and the same method (ebulloscopic, with benzene).

Table 5

Apparent Molecular Weights and Degree of  
Association of Arsenobenzene in Various Solvents

<u>Method</u>	<u>Solvent</u>	<u>Mol. Wt.</u>	<u>C<sub>6</sub>H<sub>5</sub> /molecule</u>	<u>Investigators</u>
Cryoscopic	Naphthalene	642	4.22	(3)
Ebulloscopic	Carbon bisulfide	334	2.20	(3)
Ebulloscopic	Benzene	402	2.64	(3)
Ebulloscopic	Benzene	399.8	2.63	(2)
Ebulloscopic	Benzene	915	6.02	(4)

The structure of arsenobenzene is of some biochemical interest because of the therapeutic uses to which the compound and the closely similar compound salvarsan and neosalvarsan are put. In addition, the possible presence of an arsenic-arsenic double bond in arsenobenzene is of interest in view of the fact that double bonds are seldom observed between elements in other than the first row of the periodic table. It seemed that an x-ray diffraction study, leading to a determination of the unit cell and space group of the crystal might yield useful information regarding the structure of arsenobenzene.

Preparation of Arsenobenzene Crystals

The arsenobenzene used in this investigation was prepared according to the method described by Palmer and Scott<sup>(3)</sup>.

Approximately 500 ml. of 50 weight % hypophosphorous acid was mixed with 50 g. of recrystallized phenylarsonic acid and the resulting solution stirred at 50-60°C. for about five hours under an atmosphere of carbon dioxide. At the end of this reaction time, the impure product was filtered through a Buechner funnel, washed successively with portions of warm 10% sodium hydroxide, 5% sodium hydroxide, and distilled water. It was then dried over phosphorus pentoxide, and recrystallized twice from chlorobenzene. At no time during the preparation was the material allowed to come into contact with air. The product obtained from this procedure had a melting point of 207-208°C. This compares well with previously reported values<sup>(2,3,4)</sup>, which range from 196°C. to 212°C.

In order to prepare crystals of a size suitable for x-ray and optical work, it was necessary to take care to cool the solutions slowly. Several solvents were tested of which m-xylene proved to be the most satisfactory. A few milligrams of arsenobenzene was dissolved in about 3 ml. of boiling m-xylene, and the solution was quickly poured into a previously heated 30 ml. glass weighing bottle. The weighing bottle was then stoppered and suspended in a water bath, which consisted of a Dewar flask containing water at 100°C. The Dewar flask was stoppered and allowed to cool to room temperature; the time required for the cooling was about 48 hours. No special attempt was made to keep the m-xylene

solutions free from contact with air because preliminary experiments had shown little or no evidence of oxidation under these conditions of recrystallization\*. The arsenobenzene crystals which were obtained by this procedure had a lath-like appearance, and were about 0.5 mm. long, 0.2 mm wide, and 0.1 mm. thick. Their quality for goniometric work varied, but it was on the average good. At the time when an optical examination or an x-ray photograph was to be made a suitable crystal was selected from the m-xylene solution and removed by means of a small spatula made by flattening the top of a fine wire to a thickness of about 0.01 mm. This procedure, in which the crystals were left in contact with the mother liquor until desired for use, was found to be most satisfactory because the quality of the signals obtained in the goniometry diminished appreciably after the crystal had been in contact with air for a few hours.

Crystals suitable for x-ray work were mounted on the ends of glass fibers by means of clear shallac softened by use of a hot wire. For optical work crystals were mounted with goniometer wax.

---

\* This observation is in accord with the findings of Blicke and Smith, <sup>(4)</sup> who report arsenobenzene to be more stable toward oxidation by air than had been previously supposed.

## Physical Characteristics of the Crystals

### A. Optical Examination

Arsenobenzene crystallizes in monoclinic laths with the longest dimension parallel to the two-fold axis; a drawing of a typical crystal is presented in Figure 18. Remarkably few faces were developed on the crystals. The forms  $\{100\}$  and  $\{001\}$  were found developed on almost all the crystals, but the prism faces in the same zone, such as  $(102)$ ,  $(10\bar{2})$ , and especially  $(101)$  and  $(10\bar{1})$  occurred much less frequently. Prism faces in the zone  $[100]$ , however, were found more frequently than the form  $\{010\}$ . Prism faces in the zone  $[001]$  appeared to be relatively rare.

Six crystals were examined with the optical goniometer; the approximate dimensions of these crystals were 0.5 mm. x 0.1 mm. x 0.2 mm. The reflections obtained from the faces in the zone  $[010]$  were good, although a few crystals gave double reflections from the  $(001)$  and  $(00\bar{1})$  faces. Reflections from the  $(010)$  and  $(011)$  faces were fair to good.

In Table 6 is presented a summary of the goniometric measurements and the axial ratios calculated from them.

### B. Cleavage

The crystals were found to give good cleavage parallel to the twofold axis, and appeared to have a preferred cleavage parallel to the  $(100)$  face. Attempts to cleave the crystal in other directions were for the most part unsuccessful.

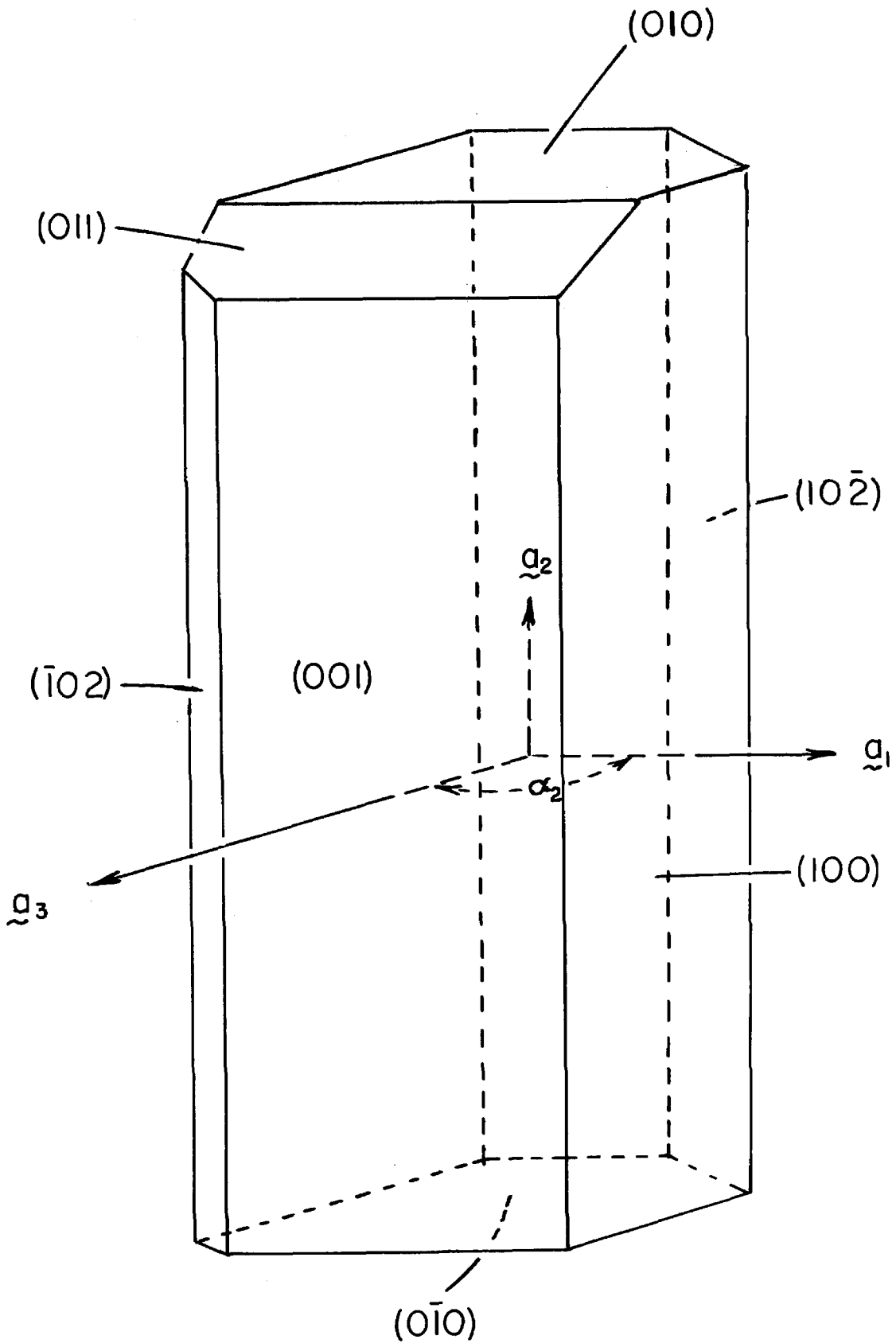


Figure 18

The Appearance of a Typical Crystal of Arsenobenzene.

Table 6

Summary of Goniometric Measurements of  
Arsenobenzene

<u>Faces</u>	<u>Number of Measurements*</u>	<u>Angles Between Aver. Value</u>	<u>the Face Normals Mean Deviation</u>
001/100	21	69°46'	11'
011/010	9	16°2'	8'
10 $\bar{2}$ /100	7	54°41'	4'

Calculated values of axial ratios and monoclinic angle

$$a_1 : a_2 : a_3 = 1.869 : 1 : 3.709$$

$$a_1 : a_3 = 0.504 : 1$$

$$\alpha_2 = = 110^\circ 14'$$

\*Number of determinations of angles between  
equivalent faces in the six crystals examined.

Determination of a Tentative Unit Cell for Arsenobenzene

A. Laue Symmetry

A Laue photograph taken with the x-ray beam parallel to the needle axis of the crystal showed the Laue symmetry of the crystal to be  $C_{2h}$ . The crystal, therefore, belongs to the monoclinic system, which confirms the conclusion drawn from goniometric measurements.

B. Layer Line Measurements

Rotation photographs were taken with each of the three crystallographic axes oriented in turn parallel to the axis of rotation.  $CuK$  radiation filtered through nickel foil was used. Measurements of the layer line separations were made and from them approximate values of the lattice constants were calculated. The results are presented in Table 7.

Table 7

Approximate Lengths of the Axes of Arsenobenzene  
as Determined by Layer Line Measurements

$$a_1 = 12.1 \overset{\circ}{\text{A}}.$$

$$a_2 = 6.24 \overset{\circ}{\text{A}}.$$

$$a_3 = 24.1 \overset{\circ}{\text{A}}.$$



### Precise Determination of Lattice Constants

Oscillation photographs of arsenobenzene were prepared with the oscillation axis parallel to each of the crystallographic axes in turn.  $\text{CuK}\alpha^*$  radiation filtered through nickel foil was used and corrections were made for shrinkage of the photographic film. The equatorial spots on each photograph were indexed, and the data from the oscillation photographs around  $a_1$  and  $a_3$  were treated by the method of least squares to obtain values for the lengths of the reciprocal axes; the angle  $\alpha_2$  was then evaluated from the lengths of the reciprocal axes and data obtained from oscillations about  $a_2$ . The results are summarized in Table 8.

### Verification of the Unit Cell

A symmetrical Laue photograph was taken with the monoclinic axis of the crystal parallel to the x-ray beam. The photograph was indexed by means of a gnomonic projection on the basis of the lattice constants given above. A total of 186 first order reflections were observed. In none of these reflections were the calculated values of  $n\lambda$  found to be less than the  $0.24 \text{ \AA}$ , the short wave length limit.

---

\* The wave lengths employed in the calculations were in Angströms and are as follows:  $\text{CuK}\alpha_1 = 1.54050$ ,  $\text{CuK}\alpha_2 = 1.54434$ ,  $\text{CuK}\alpha = 1.54180$ .

Table 8

Precise Determination of Lattice Constants  
for Arsenobenzene

A. Calculation of  $b_1$  and  $b_2$

Index of spot $h_1h_2h_3$	$\frac{2 \sin \vartheta}{\lambda}$ observed	$\frac{2 \sin \vartheta}{\lambda}$ calculated	$\frac{h_1h_20(\text{calc})}{h_1h_20(\text{obs})}$	Weighting factor*
100	0.0882	0.0876	0.993	1
200	0.1764	0.1753	0.993	1
300	0.2642	0.2629	0.995	2
410	0.3873	0.3856	0.996	2
510	0.4693	0.4667	0.994	2
520	0.5422	0.5435	1.002	2
620	0.6182	0.6164	0.997	3
720	0.6949	0.6919	0.996	4
630	0.7154	0.7135	0.997	5
730	0.7826	0.7803	0.997	5
830	0.8528	0.8509	0.998	5
930	0.9262	0.9245	0.998	5
840	0.9524	0.9515	0.999	5
560**	{ 1.0594	1.0596	1.000	5
	{ 1.0699		1.000	5
660**	{ 1.0985	1.0985	1.000	5
	{ 1.0979		1.001	5
370**	{ 1.1548	1.1556	1.001	3
	{ 1.1558		1.000	3
470**	{ 1.1772	1.1786	1.001	3
	{ 1.1781		1.000	3
860**	{ 1.1924	1.1923	1.000	3
	{ 1.1935		0.999	3
		Average	0.999	

\*\*\*

$$b_1 = 0.0876 \pm 0.0001 \text{ \AA}^{-1}$$

$$b_2 = 0.1607 \pm 0.0002 \text{ \AA}^{-1}$$

\* The weighting factor applied was selected by considerations of the quality of the reflection and the relative magnitude of  $\frac{2 \sin \vartheta}{\lambda}$ .

\*\* The  $\alpha_1 \alpha_2$  doublet was resolved in these reflections.

\*\*\* The limits of error were established by considering the average deviation in  $h_{\text{calc}}/h_{\text{obs}}$  as due entirely to errors in the lengths of each of the reciprocal axes in turn.

Table 8 (Continued)

B. Calculation of  $b_3$  and  $b_2$

Index of spot $h_1h_2h_3$	$\frac{2 \sin \psi}{\lambda}$ observed	$\frac{2 \sin \psi}{\lambda}$ calculated	$\frac{h_1h_2O(\text{calc})}{h_1h_2O(\text{obs})}$	Weighting Factor
006	0.2668	0.2661	0.997	1
018	0.3908	0.3898	0.997	1
019	0.4316	0.4301	0.997	1
0.1.10	0.4735	0.4716	0.996	1
0.1.12	0.5574	0.5566	0.999	1
0.1.13	0.6000	0.5983	0.997	1
0.2.12	0.6234	0.6216	0.997	2
0.1.14	0.6422	0.6412	0.998	2
0.2.14	0.7006	0.6991	0.998	3
0.3.12	0.7198	0.7181	0.998	3
0.2.15	0.7404	0.7387	0.998	3
0.2.16	0.7801	0.7788	0.998	3
0.3.14	0.7882	0.7861	0.997	4
0.4.12	0.8359	0.8345	0.998	4
0.3.16	0.8596	0.8578	0.998	4
0.4.13	0.8647	0.8635	0.999	5
0.4.14	0.8953	0.8993	1.004	5
0.5.10	0.9179	0.9179	1.000	5
0.4.15	0.9261	0.9250	0.999	5
0.3.16	0.9336	0.9324	0.999	5
0.5.11	0.9408	0.9401	0.999	5
0.4.16	0.9584	0.9574	0.999	5
0.5.13	0.9909	0.9890	0.998	5
0.4.18	1.0238	1.0257	1.002	5
0.6.9	1.0437	1.0437	1.000	5
0.6.10	1.0610	1.0615	1.000	5
0.6.12	1.1018	1.1015	1.000	5
0.6.14	{ 1.1463	1.1470	1.001	5
	{ 1.1470		1.001	5
0.6.16	{ 1.1963	1.1973	1.001	5
	{ 1.1966		1.001	5
0.7.11	{ 1.2251	1.2264	1.001	5
	{ 1.2252		1.001	5
Average			1.000	

$$b_3 = 0.0443 \pm 0.00006 \text{ \AA}^{-1}$$

$$b_2 = 0.1606 \pm 0.0002 \text{ \AA}^{-1}$$

Table 8 (Continued)

C. Calculation of  $\beta_2$  from  $b_1$  and  $b_3$  and  $h_10h_3$  reflections

Index of spot $h_1h_2h_3$	$\frac{2 \sin \vartheta}{\lambda}$	$\cos \beta_2$
402	0.3305	0.3473
604	0.4934	0.3458
808	0.6671	0.3462
5.0.10	0.7219	0.3410
9.0.10	0.7592	0.3462
9.0.12	0.7840	0.3461
4.0.14	0.8109	0.3433
10.0.12	0.8532	0.3466
10.0.14	0.8812	0.3464
4.0.16	0.8918	0.3398
10.0.16	0.9169	0.3463
10.0.18	0.9590	0.3468
11.0.16	{ 0.9789	0.3468
	{ 0.9793	0.3462
10.0.20	{ 1.0079	0.3466
	{ 1.0078	0.3466
11.0.20	{ 1.0617	0.3441
	{ 1.0612	0.3432
10.0.24	{ 1.1195	0.3469
	{ 1.1199	0.3464
10.0.26	{ 1.1813	0.3472
	{ 1.1813	0.3471
11.0.18	{ 1.0160	0.3470
	{ 1.0158	0.3472

Average value  $\cos \beta_2$  = 0.3457

Calculated value of  $\beta_2$  =  $69^{\circ}46'$

Average deviation =  $5'$

Table 8 (Continued)

D. Summary

$$b_1 = 0.0876 \pm 0.0001 \text{ \AA}^{-1}$$

$$b_2 = 0.1606 \pm 0.0002 \text{ \AA}^{-1}$$

$$b_3 = 0.0443 \pm 0.00006 \text{ \AA}^{-1}$$

$$\beta_2 = 69^{\circ}46' \pm 5'$$

The unit cell dimensions

$$a_1 = 12.16 \pm 0.02 \text{ \AA}$$

$$a_2 = 6.22 \pm 0.01 \text{ \AA}$$


$$a_3 = 24.10 \pm 0.08 \text{ \AA}$$

$$\alpha_2 = 110^{\circ}14' \pm 5'$$

$$a_1 : a_2 : a_3 = 1.955 : 1 : 3.875$$

$$a_1 : a_3 = 0.505 : 1$$

Number of Molecules of Arsenobenzene per Unit Cell

The density of the crystals of arsenobenzene was determined by the suspension method. Carbon tetrachloride was added to a number of crystals of arsenobenzene placed in the tip of a centrifuge tube, and the density of this liquid medium was varied by the addition of ethylene dibromide until the heaviest crystals remained suspended under centrifugation. The density of the resulting solution was found to be 1.812 g/cc. by means of a pycnometer. From this the number of monomeric arsenobenzene units ( -As ) per unit cell is found to be 12 (12.3 calculated).

Determination of the Space Group of Arsenobenzene

Weissenberg photographs were made of the equator, and of the first and second layer lines with  $a_2$  oriented parallel to the axis of rotation, and of the equator with  $a_3$  parallel to the axis of rotation. The photographs were indexed with the aid of an indexing chart and the reflections were tabulated. Pertinent data from these photographs are presented in Table 9. Since the reflections ( $h_10h_3$ ) with  $h_3$  odd do not appear, a  $C$  glide plane is indicated to be a symmetry element of the arsenobenzene crystal. The presence of a twofold screw axis, which requires extinctions of the type  $0h_20$  with  $h_2$  odd, is ruled out by the appearance of the reflections (010) and (030). The extinction rules required by centered lattices are also violated.

Table 9. Data from Weissenberg Photographs

A. Reflections and absences from $h_1$ ohz		$00h_3$	$10h_3$	$20h_3$	$30h_3$	$40h_3$	$50h_3$	$60h_3$	$70h_3$	$80h_3$	$90h_3$	$10.0.h_3$	$11.0.h_3$	$12.0.h_3$
$h_1$	$h_3$													
$h_1$	00			200	300		500	600	700	800	900	10.0.0	11.0.0	12.0.0
$h_1$	02		102	202				602	702	802		10.0.2	11.0.2	12.0.2
$h_1$	04		104	204				604	704	804				
$h_1$	06			206		406	506	606	706	806				
$h_1$	08			208	308	408		608	706	808				
$h_1$	0.10		1.0.10	2.0.10	3.0.10	4.0.10	5.0.10		7.0.10					
$h_1$	0.12		1.0.12	2.0.12	3.0.12	4.0.12	5.0.12							
$h_1$	0.14					4.0.14								
$h_1$	0.16		1.0.16	2.0.16	3.0.16									
$h_1$	0.18		1.0.18	2.0.18										
$h_1$	02			202		402		602	702	802			11.0.2	12.0.2
$h_1$	04			204	304	404	504	604				10.0.6	11.0.6	
$h_1$	06		106	206	306	406	506		706	806	906		11.0.8	
$h_1$	08		108	208	308	408	508		708	808	908			
$h_1$	0.10		1.0.10	2.0.10	3.0.10	4.0.10	5.0.10	6.0.10	7.0.10	8.0.10	9.0.10	10.0.10		
$h_1$	0.12		1.0.12	2.0.12	3.0.12	4.0.12	5.0.12	6.0.12	7.0.12	8.0.12	9.0.12	10.0.12		
$h_1$	0.14		1.0.14	2.0.14	3.0.14	4.0.14	5.0.14	6.0.14	7.0.14					
$h_1$	0.16		1.0.16	2.0.16	3.0.16	4.0.16	5.0.16	6.0.16		8.0.16	9.0.16			
$h_1$	0.18		1.0.18	2.0.18	3.0.18	4.0.18	5.0.18	6.0.18		8.0.18	9.0.18	10.0.18		
$h_1$	0.20		1.0.20	2.0.20			5.0.20	6.0.20	7.0.20	8.0.20	9.0.20	10.0.20		
$h_1$	0.22		1.0.22		3.0.22	4.0.22	5.0.22	6.0.22	7.0.22					
$h_1$	0.24		1.0.24	2.0.24	3.0.24									

B. Orders from  $Oh_2O$  observed: 010, 020, 030, 040.

The information given by the x-ray experiments serves to eliminate all of the space groups except  $C_{2h}^1 - P_m^2$ ,  $C_{2h}^4 - P_c^2$ ,  $C_2^1 - P_2$ ,  $C_s^1 - P_m$ , and  $C_s^2 - P_c$ . If a  $c$  glide plane is present, as seems certain from the observed extinctions, the probable space groups are  $C_{2h}^4 - P_c^2$  and  $C_s^2 - P_c$ . No attempt has been made to determine whether or not the crystal has a center of symmetry, which would permit a choice between these two space groups.

#### Summary of Work on Arsenobenzene

The results of the work on arsenobenzene is presented in Table 10.

The agreement between the axial ratios calculated from x-ray and optical measurements is not as good as is usually obtained. This appears to be due to the large ratio of  $a_3/a_2$  in the arsenobenzene crystal and to the difficulty of getting sharp, clean reflections from the (011) face. It is found that this difference in axial ratios represents an error of only about  $\frac{1}{2}^\circ$  in the (011)/(010) angle. For this reason, we do not consider this disagreement to be disturbing. The ratio  $a_1/a_3$ , which is very much less sensitive to changes in the angles measured by goniometry, is found to be in excellent agreement with the result from the x-ray experiments.

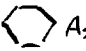


Table 10

Summary of Work on Arsenobenzene


Probable Space Groups	$C_{2h}^4 - P_c^2$ or $C_s^2 - P_c$	
Lattice Constants		
$a_1$	$12.16 \pm 0.02 \text{ \AA}.$	
$a_2$	$6.22 \pm 0.01 \text{ \AA}.$	
$a_3$	$24.10 \pm 0.08 \text{ \AA}.$	
	$110^\circ 14' \pm 5'$	
Density in $\text{g./cm}^3$ at $26.4^\circ\text{C}$	1.812	
Number of $\text{C}_6\text{As}$ units per unit cell.	12 (12.3 calc.)	
Axial ratios and monoclinic angle	x-ray	optical
$a_1 : a_2 : a_3$	1.955 : 1 : 3.875	1.869 : 1 : 3.709
$a_1 : a_3$	0.505 : 1	0.504 : 1
	$110^\circ 14'$	$110^\circ 14'$

Discussion

The space group and unit cell of the arsenobenzene crystal do not give as much information regarding the structure of the molecule as had been hoped for at the outset of this investigation. Provided that there is only one kind of molecule present, the 12  As units may be combined so as to give 1, 2, 3, 4, 6 or 12 molecules consisting of 12, 6, 4, 3, 2, or 1 of these units respectively. Since it is extremely unlikely that arsenic should form only one bond, the possibility of 12 molecules of 1 unit each may be excluded. Neither 1 molecule of 12 units nor 3 molecules of 4 units each is compatible with the presence of a glide plane. There remains to be considered only the possibility of 6 molecules of 2 units each, 4 molecules of 3 units or 2 molecules of 6 units.

In addition to the discrete molecule mentioned above, however, there exists the very interesting possibility that arsenobenzene crystallizes with the arsenic atoms bonded together in infinite chains, probably parallel to the monoclinic axis. Such a structure is possessed by crystalline selenium, which is adjacent to arsenic in the periodic table; and it is not unreasonable to suppose that arsenic (which in the elementary state crystallizes with the atoms bonded together in infinite sheets) could also form infinite chains after saturation of some of its side valences as occurs in

arsenobenzene. This type of structure provides a satisfactory explanation for several of the properties of arsenobenzene, both in the crystalline state and in solution; for example:

- (1) Cleavage of the crystal occurs with marked ease parallel to the monoclinic axis of the crystal.
- (2) Oscillation and rotation photographs made with the monoclinic axis of the crystal parallel to the rotation axis show a marked falling off in the intensity of the spots from low to high angles of scattering. This effect is not observed in the photographs made by rotation or oscillation of the crystal about the other axes, and may be interpreted as a temperature effect resulting from the relatively greater freedom of motion in directions other than that parallel to the chains.
- (3) The wide variation in the results of the determinations of the molecular weight of arsenobenzene is not hard to understand if the  units are bonded together in infinite chains. The size of the chain fragments in a solution of arsenobenzene would be expected to vary with the conditions under which it was dissolved, and if the equilibria between these several species is slow, fluctuations in the average molecular weight would result.

- (4) The chain structure is in accord with the general observation regarding the formation of only single bonds between elements in other than the first row of the periodic table.

If arsenobenzene does have a structure composed of infinite chains of  $\langle \text{C}_6\text{H}_5 \rangle_{\text{As}}$  units, arranged parallel to the two-fold axis, it is likely that the unit cell contains either two or four of such chains. Six chains permit only two arsenic atoms per chain to be contained in a distance of 6.22 Å. (the length of the two-fold axis), which requires an arsenic-arsenic bond distance of 3.11 Å. at a bond angle of 180°. The normal bond distance is about 2.4 Å. and the bond angle about 97°. In the case of 4 chains the bond angle is calculated to be about 120° (based on an arsenic-arsenic distance of 2.4 Å.) which is still very much larger than normal.

We intend to continue the investigation of this structure. The positions of the arsenic atoms may be obtained by Patterson projections, and it is hoped that further refinement can be made by Fourier methods.

References

- (1) A. Michaelis and C. Schults, Ber., 14 912 (1881).
- (2) A. Michaelis and A. Schafer, Ber., 46 1742 (1913).
- (3) C. S. Palmer and A. B. Scott, Jour. Am. Chem. Soc.,  
50, 536 (1928).
- (4) F. F. Blicke and F. D. Smith, ibid., 52 2946 (1930).

Propositions Submitted by Kenneth W. Hedberg

Ph.D. Oral Examination, May 28, 1948, 9:00 A.M., Crellin Conference Room  
Committee: Dr. Corey, (Chairman), Professors Badger, Bates, Lauritsen,  
Lucas, Sturdivant, and Dr. Waser.

1. The surprising and astonishingly incorrect structure obtained by Bastiansen and Hassel (1) for 1,3,5,7-cyclooctatetraene cannot have resulted from the normal uncertainties of the electron diffraction method. I propose that the explanation of this result lies in the interpretation by these investigators of the diffraction pattern of styrene as that of cyclooctatetraene.

(1) See O. Bastiansen, O. Hassel, and A. Sangseth,  
Nature, 160, 128 (1947)

2. (a) The procedure employed by Staudinger and Rheiner (2) for the isolation of  $\beta$ -dicyclopentadiene cannot have resulted in the separation of this stereoisomer.

(b) It seems quite possible that  $\beta$ -dicyclopentadiene does not exist. I propose that appropriately treated samples of dicyclopentadiene be subjected to chromatographic experiments in an attempt to settle this point by separation of the proposed  $\alpha$ - and  $\beta$ -isomers.

(2) H. Staudinger and A. Rheiner, Helv. Chim. Acta,  
7, 23 (1924)

3. Structural formulas frequently written for molecules of trivalent arsenic compounds in which an arsenic atom is represented as doubly bonded to another atom are misleading in the impression they are intended to convey regarding the structure of these molecules.

4. The conclusion of Jagger (3) regarding the probable identity of the gases contained in parent magmas is not in accord with the theory of the temperature in volcanic hearths.

(3) T. A. Jagger, Am. Jour. Sci., 238, 311 (1940)

5. (a) Cyclooctatetraene, a golden yellow liquid at room temperature, forms colorless crystals when cooled to  $-7.5^{\circ}\text{C}$ . It has been suggested (4) that this change of color on cooling is due to the disappearance of a diradical species. If this change in color is actually a characteristic of cyclooctatetraene, I propose that a more reasonable explanation would involve the disappearance of monomer as a result of polymerization.

(b) Experiments are proposed which should be of value in solving this problem.

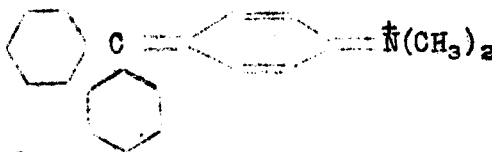
(4) R. C. Pink and H. R. Ubbelohde, Nature, 160, 502 (1948)

6. The I.B.M. machines and the file of Gaussian error function punched cards in this laboratory could be applied to the analysis of molecular spectra (such as vibrational or electronic spectra in the condensed phase) to give relatively accurate values for the absorption frequencies and for their intensities.
7. The determination of the structure of diborane by Bauer (5), contrary to this author's assertion, should not be considered good evidence in favor of an ethane-like model for this molecule as opposed to a bridge model.

(5) S. H. Bauer, Jour. Am. Chem. Soc., 59, 1096 (1937)

8. I propose that it would be interesting to study the following chemical reactions in connection with the work described in part I of this thesis

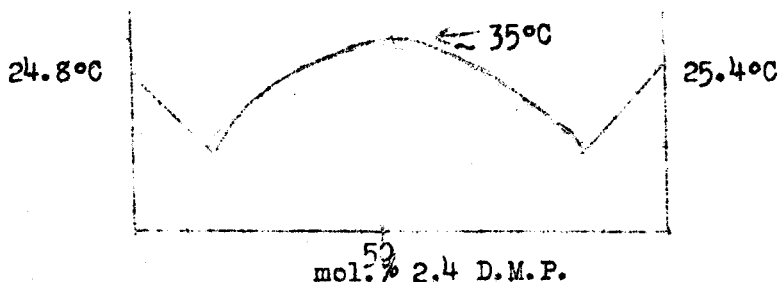
(a) the rate of formation of crystal violet dye from crystal violet carbinol, and also the rate of formation of the dye



from its carbinol.

(b) the oxidation of leuco malachite green and/or leuco crystal violet with ammonium hexanitrate cerate in nitric acid and with ceric perchlorate in perchloric acid solution.

- (a)  
9. The phase diagram of 2,4-dimethyl phenol and 2,4-dimethyl-6-tert. butyl phenol has the following approximate appearance:



I propose that the explanation of the broad rounded hump with maximum at approximately 50 mol. % 2,4-dimethyl phenol results from the formation of a compound brought about by unusually strong hydrogen bonding

(b) Studies of the absorption spectrum of this system in the infra-red should be made.

11. The practice of submitting a "bull" proposition as a tenth proposition should be discontinued.